

Enhancing biodiversity through intraspecific suppression in large ecosystems

Seong-Gyu Yang (양성규)^{1,2} and Hye Jin Park (박혜진)^{3,*}

¹*School of Computational Sciences, Korea Institute for Advanced Study, Seoul, 02455, Republic of Korea*

²*Asia Pacific Center for Theoretical Physics, Pohang, 37673, Republic of Korea*

³*Department of Physics, Inha University, Incheon 22212, Republic of Korea*

(Dated: April 2, 2024)

The competitive exclusion principle (CEP) is a fundamental concept in the niche theory, which posits that the number of available resources constrains the coexistence of species. While the CEP offers an intuitive explanation on coexistence, it has been challenged by counterexamples observed in nature. One prominent counterexample is the phytoplankton community, known as the paradox of the plankton. Diverse phytoplankton species coexist in the ocean even though they demand a limited number of resources. To shed light on this remarkable biodiversity in large ecosystems quantitatively, we consider *intraspecific suppression* into the generalized MacArthur's consumer-resource model and study the relative diversity, the number ratio between coexisting consumers and resource kinds. By employing the cavity method and generating functional analysis, we demonstrate that, under intraspecific suppression, the number of consumer species can surpass the available resources. This phenomenon stems from the fact that intraspecific suppression prevents the emergence of dominant species, thereby fostering high biodiversity. Furthermore, our study highlights that the impact of this competition on biodiversity is contingent upon environmental conditions. Our work presents a comprehensive framework that encompasses the CEP and its counterexamples by introducing intraspecific suppression.

AUTHOR SUMMARY

The niche theory addresses the challenge of understanding how ecological communities are formed and sustained by explaining species' coexistence based on their ecological niches. When species share identical niches, they cannot coexist, which is known as the competitive exclusion principle (CEP). However, observations in phytoplankton communities contradict the CEP, presenting a paradox. Various mechanisms, such as temporal fluctuations and spatial heterogeneity, have been proposed to resolve this paradox. Here, we introduce intraspecific suppression as a novel mechanism to reconcile this paradoxical scenario and understand coexistence comprehensively. Our model incorporates intraspecific suppression and shows its potential to enhance biodiversity beyond CEP prediction. In addition, we highlight the crucial role of environmental conditions in utilizing intraspecific suppression to significantly elevate biodiversity, surpassing the limits set by the CEP. Through these insights, we deepen our understanding of the factors influencing species coexistence.

INTRODUCTION

Understanding how ecological communities are assembled and maintained is a challenging problem in ecology. A prominent theory developed to explain the coexistence of diverse species is the *niche* theory [1]. The ecological niche refers to all the environmental factors required for a species' survival, such as resources and habitat. According to the competitive exclusion principle (CEP) [2], if two species have identical niches, they cannot coexist in the same ecological community. Therefore, there needs to be a niche differentiation among species for coexistence. The more species assemble in an ecological community, however, the more overlap in their niche is inevitable, which limits the number of coexisting species in a given environment. The CEP has been supported by the experimental observations on the coexistence of unicellular organisms [3, 4] and the observations on warblers [5]. Theoretical studies have demonstrated the CEP by showing that the number of coexisting species cannot exceed the number of available resource kinds [6–8].

Even though the CEP furnishes an intuitive explanation in the assemblage of ecological communities, counterexamples of the CEP have been found in nature. One such example is observed in the ocean with phytoplankton, known as the *paradox of the plankton* [9]. Phytoplankton species consume a limited number of resources. Despite this constraint, the phytoplankton community displays a remarkable diversity, with a greater number of species than the

* hyejin.park@inha.ac.kr

available resource kinds [10–12]. To explain the biodiversity exceeding the bound that the CEP predicts, temporal environmental fluctuations, spatial heterogeneity, and other mechanisms have been proposed [9, 13, 14] and provided successful explanations. To address the paradox within the niche theory and explain the coexistence of diverse species, we introduce *intraspecific suppression* as a novel mechanism, which is known for its capacity to enhance the stability of large ecological systems [15, 16]. Intraspecific suppression represents not only a direct competition among individuals of the same species such as fights for potential mates but also the growth suppression by pathogen spreading within the same species through contact [14, 17] such as in the Kill the Winner hypothesis [18–21].

We develop our model based on MacArthur’s consumer-resource model (MCRM) [22–24] where the CEP holds. The MCRM describes a system in which resource species experience logistic growth while consumer species compete for these shared resources. Consequently, the resources act as ecological niches, and the number of coexisting consumer species cannot exceed the number of available resources. In a recent study, W. Cui and colleagues extended the MCRM by considering externally supplied resources [25]. Even though resources are externally supplied such that resource species never go extinct, the calculated bound of coexisting consumer species cannot explain the paradox of the plankton in the generalized MCRM (GCRM).

By incorporating intraspecific suppression into GCRM, we investigate the role of intraspecific suppression on consumer diversity and comprehend the paradox of the plankton. The interactions between consumers and resources are considered random, which allows us to describe large ecological systems systematically, akin to R. May’s research [26]. By employing techniques from statistical physics to handle the quenched disorder interaction [25, 27, 28], we examine the steady-state solution of the system and obtain the abundance distributions of consumers and resources. The results show that intraspecific suppression enhances consumer diversity and can even further increase biodiversity beyond the CEP bound for large ecological systems, embracing the paradox within a competition-based framework. Furthermore, we found that biodiversity beyond the CEP bound arises only when the resource is rich enough, addressing the condition where intraspecific suppression acts as an additional limiting factor.

MODEL

The GCRM describes the abundance dynamics of ecological systems consisting of S different consumer species and M different kinds of resources [25]. We focus on the externally supplied resources as illustrated in Fig 1. The case for the self-renewing resources that exhibits the logistic growth is discussed in Sec. C. Introducing the intraspecific suppression in the GCRM, we write the abundance dynamics of consumers and resources as follows:

$$\begin{aligned}\dot{N}_i &= N_i \left(\sum_{\alpha} C_{i\alpha} R_{\alpha} - m_i - h_i N_i \right), \\ \dot{R}_{\alpha} &= K_{\alpha} - \left(D_{\alpha} + \sum_i N_i C_{i\alpha} \right) R_{\alpha},\end{aligned}\tag{1}$$

where N_i and R_{α} denote the abundance of consumer i ($= 1, 2, \dots, S$) and resource α ($= 1, 2, \dots, M$), respectively. Consumer i grows by taking resource α with a consumption rate $C_{i\alpha}$ and dies with a mortality rate m_i . The resource α is externally supplied with an input rate K_{α} and degraded with a degradation rate D_{α} . The last term in the consumer abundance dynamics is the intraspecific suppression term, and h_i indicates an intraspecific suppression coefficient of consumer i .

To describe large ecological systems, the number of consumer species S and resource kinds M are assumed to be infinitely large ($S, M \rightarrow \infty$), but with a finite ratio $\gamma (\equiv M/S)$. At a steady state, some species could go extinct, and only S^* ($\leq S$) surviving consumer species coexist. On the contrary, resources never go extinct due to the external supply, and thus the number of available resources $M^* = M$.

Since we consider the infinitely large system, assigning all the values of $C_{i\alpha}$ is unfeasible. In this situation, using a random matrix is a good option to systematically describe the interactions for theoretical approaches [25–35]. The values of $C_{i\alpha}$ are randomly drawn from the Gaussian distribution $\mathcal{N}(\mu_C/M, \sigma_C^2/M)$ with the mean μ_C/M and variance σ_C^2/M . Other parameters such as m_i , K_{α} , and D_{α} are also independently drawn from Gaussian distributions with means m , K , and D , respectively. The standard deviation of a parameter X is denoted by σ_X . We fix the parameters $\mu_C = 1$, $m = 1$, $D = 1$, $\sigma_m = 1/10$, $\sigma_D = 0$, and $\sigma_K = 1/10$ throughout this study. For the sake of simplicity, we set $h_i = h$ for all i , i.e., $\sigma_h = 0$. The general study for nonzero σ_h is addressed in Sec. A.

Large ecological systems with the quenched disorder in interactions have been studied using the cavity method [36–38] and the generating functional analysis [39–43]. These approaches assume that all the consumer species follow the same rule, and as do the resources. Consequently, all consumer species adhere to a single abundance distribution, denoted as $P(N)$, and all resource species follow a abundance distribution, denoted as $P(R)$. We theoretically obtain

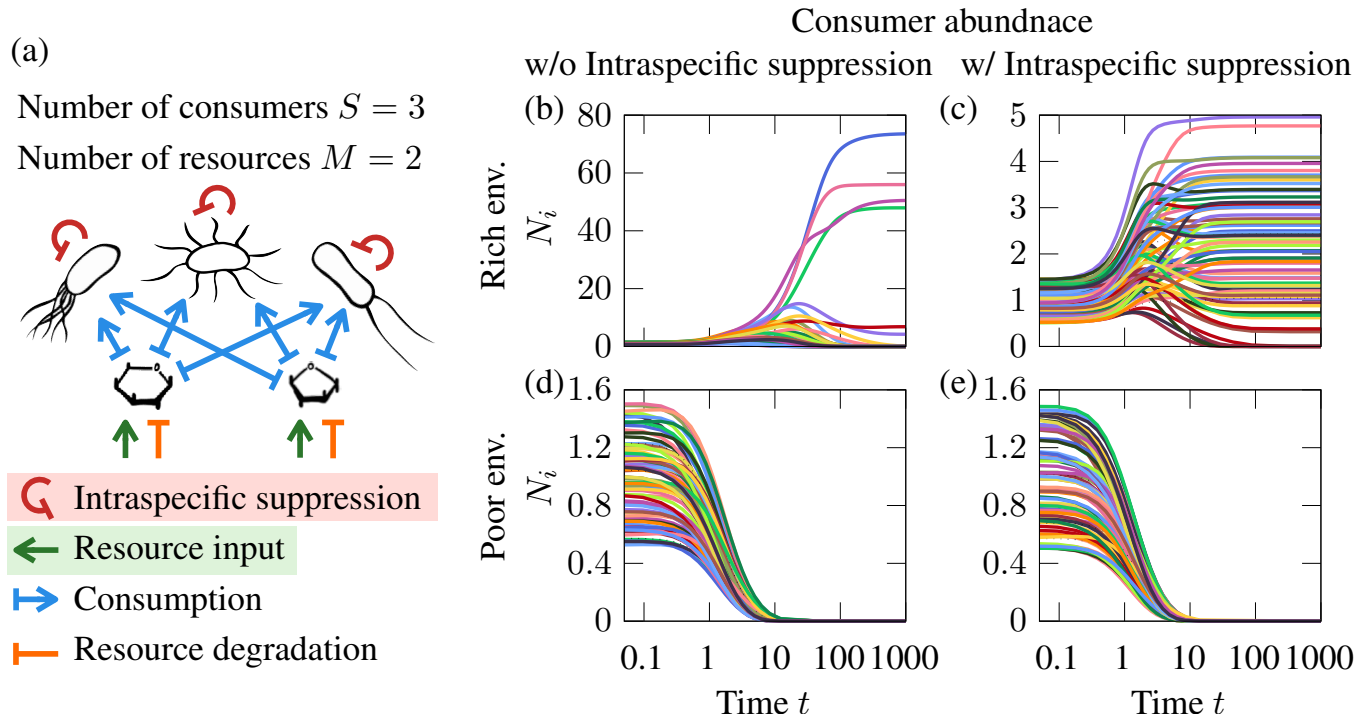


FIG. 1. (a) Schematic figure of an ecological system that consists of three consumer species ($S = 3$) and two resource kinds ($M = 2$). Three bacteria species consume two different monosaccharide resources, and the resources are externally supplied. Blue straight arrows denote the resource consumption, and red circular arrows indicate intraspecific suppression. Orange and green straight arrows denote the degradation and the external resource supply, respectively. For all arrows, the abundance growth of agents at the sharp end (\rightarrow) is stimulated, and that at the blunt end (\leftarrow) is suppressed. [(b)–(e)] Dynamics of consumer abundances in ecosystems with $S = 75$ and $M = 50$. In rich environments (b) and (c), intraspecific suppression has the potential to enhance biodiversity. However, in poor environments (d) and (e), interspecific suppression alone without sufficient resources cannot sustain high levels of diversity.

the expressions of consumer abundance distribution $P(N)$ and resource abundance distribution $P(R)$ in terms of macroscopic quantities; surviving probability of consumers $\phi_S (= S^*/S)$, average consumer abundance $\langle N \rangle$, average squared consumer abundance $\langle N^2 \rangle$, consumer's response $\nu (= -\langle \partial N / \partial m \rangle)$, average resource abundance $\langle R \rangle$, average squared resource abundance $\langle R^2 \rangle$, and resource's response $\chi (= -\langle \partial R / \partial D \rangle)$ (see details in Sec. A). Those macroscopic quantities depend on themselves, giving self-consistent equations. Solving those self-consistent equations, we evaluate the macroscopic quantities and obtain the distributions $P(N)$ and $P(R)$.

We investigate consumer abundances at the steady state and examine the impact of intraspecific suppression and environmental conditions on their diversity (see Fig. 1). In the presence of intraspecific suppression, consumers are unable to attain large abundances, thereby leading to an increase in the number of small consumer communities and enhancing diversity, particularly in resource-rich environments. However, this effect diminishes in resource-scarce environments, where species struggle to meet minimum energy requirements. Through theoretical derivation of the ratio S^*/M^* and numerical integration of Eq. 1, we rigorously investigate these scenarios and present our findings in the following section.

RESULTS

Intraspecific suppression enhances biodiversity beyond the CEP bound

To study how many consumer species coexist, we measure the relative diversity S^*/M^* , which is the number ratio between coexisting consumers and available resources at the steady state. By definition, S^*/M^* is equal to $\gamma^{-1}\phi_S$, where ϕ_S is the surviving probability S^*/S and the number of resources remains still $M^* = M$ for externally supplied

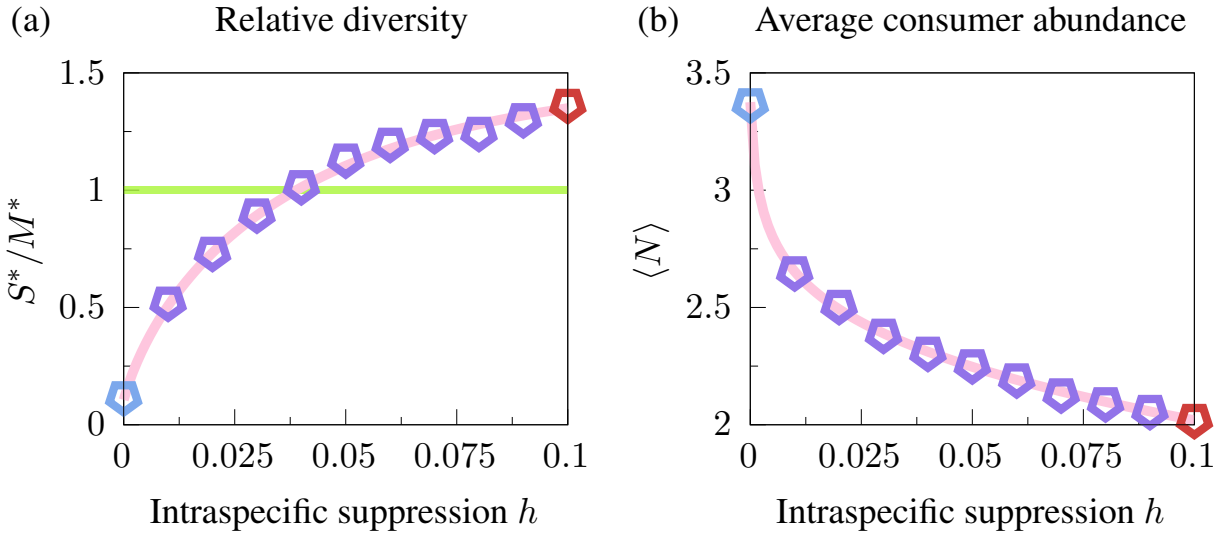


FIG. 2. (a) Relative diversity S^*/M^* and (b) average consumer abundance $\langle N \rangle$ against intraspecific suppression coefficient h for fixed ratio $\gamma = M/S = 2/3$. The pink lines denote the theoretical results with assumptions of large numbers of consumer species and resource kinds ($S, M \rightarrow \infty$). The symbols denote the numerical simulation results averaging over 50 independent realizations for $S = 75$ and $M = 50$. The solid chartreuse line in (a) indicates the bound of S^*/M^* suggested in the CEP. As intraspecific suppression becomes stronger, the relative diversity increases and even exceeds the CEP bound, while the average consumer abundance decreases. The blue and red symbols denote the results for $h = 0$ and $h = 1/10$, respectively. The error bars are smaller than the symbol size. We used the consumption rate deviation $\sigma_C = 1/10$ and the average resource input rate $K = 5$.

resources. We mainly vary h to investigate the effect of intraspecific suppression on the relative diversity S^*/M^* . Our theoretical results reveal that $\phi_S = h_{\text{eff}}\nu$, where $h_{\text{eff}} (\equiv h + \sigma_C^2\chi)$ is the effective intraspecific suppression coefficient (detailed derivations are presented in Sec. A). Thus, we obtain $S^*/M^* = \gamma^{-1}\phi_S = \gamma^{-1}h_{\text{eff}}\nu$. As shown in Fig 2(a), as intraspecific suppression h increases, the diversity S^*/M^* raises. It is because intraspecific suppression subdues the population growth of consumer species, as shown in Fig 2(b), and thus any dominant species are hard to emerge, resulting in many coexisting species with small abundances. When intraspecific suppression is significantly elevated, this effect is notably intensified, leading to the relative diversity S^*/M^* that exceeds 1, thereby surpassing the bound predicted by the CEP and resolving the plankton paradox. It means that the introduction of intraspecific suppression allows us to embrace the paradox within a competition-based scheme.

As the surviving probability ϕ_S can be calculated from the consumer abundance distribution $P(N)$, we can understand the behavior of the relative diversity S^*/M^* in terms of $P(N)$. The consumers with zero abundance ($N = 0$) are considered extinct, and thus only consumers with $N > 0$ contribute to the number of coexisting consumers S^* , and the surviving probability ϕ_S is estimated by integrating the consumer abundance distribution $P(N)$ over $N > 0$, i.e., $\phi_S = \int_{+0}^{\infty} P(N)dN$. We theoretically derive $P(N)$ as the truncated Gaussian distribution $\max(0, z)$, where the function $\max(x, y)$ returns the larger value between x and y , and the random variable z follows the Gaussian distribution $\mathcal{N}(g_{\text{eff}}/h_{\text{eff}}, \sigma_g^2/h_{\text{eff}}^2)$. Here, $g_{\text{eff}} (= \mu_C \langle R \rangle - m)$ and $\sigma_g (= \sqrt{\sigma_m^2 + \sigma_C^2 \langle R^2 \rangle})$ denote the average consumer growth rate without explicit intraspecific suppression and the deviation in consumer growth rate, respectively (see Fig. 3). If the average growth rate g_{eff} is zero, half of the consumers survive as only half of them have positive abundance by chance. As g_{eff} increases, more consumers have positive abundances, inducing higher consumer diversity. In the case of positive g_{eff} , a large σ_g induces further extinction, reducing the diversity, while the effect of σ_g is the opposite for negative g_{eff} ; the larger the σ_g , the more consumers coexist. Altogether, g_{eff} and σ_g determine the relative diversity S^*/M^* . Using the expression $S^*/M^* = \gamma^{-1} \int_{+0}^{\infty} P(N)dN$, we obtain

$$S^*/M^* = \frac{\gamma^{-1}}{2} \left[1 + \text{erf} \left(\frac{g_{\text{eff}}}{\sqrt{2}\sigma_g} \right) \right], \quad (2)$$

where $\text{erf}(x)$ denotes the error function. The relative diversity S^*/M^* exhibits a monotonic increase with g_{eff}/σ_g .

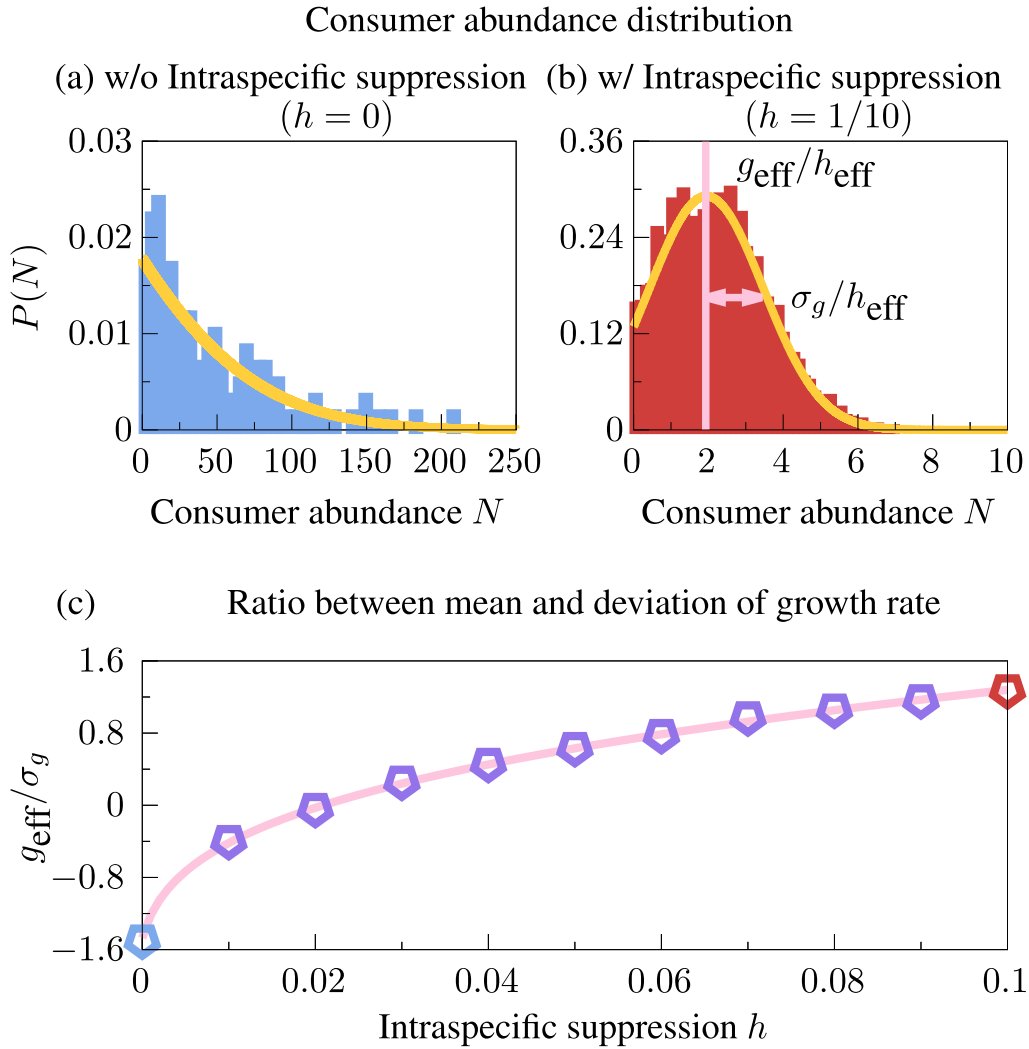


FIG. 3. Consumer abundance distribution $P(N)$ for $N > 0$ (a) without ($h = 0$) and (b) with ($h = 1/10$) intraspecific suppression. The distribution $P(N)$ exhibits the truncated Gaussian distributions for both cases. The peak position and the width of the Gaussian distributions are determined by $g_{\text{eff}}/h_{\text{eff}}$ and σ_g/h_{eff} , respectively. The probability of extinct consumer species ($N = 0$) is not shown here. (c) Ratio between mean and width g_{eff}/σ_g versus h . As h increases, g_{eff}/σ_g increases, which indicates that the strong intraspecific suppression increases the relative diversity S^*/M^* (see the main text). We used the deviation of consumption rate $\sigma_C = 1/10$ and the resource input rate $K = 5$.

Consequently, the increase in S^*/M^* with h is attributed to the rise in g_{eff}/σ_g with h , as depicted in Fig 3(c). The underlying mechanism is as follows: Intense intraspecific suppression leads to reduced consumer abundance, thereby yielding higher average resource abundance. From the definition of $g_{\text{eff}} (= \mu_C \langle R \rangle - m)$, we can see that the elevated average resource abundance contributes to the increase in g_{eff} . This result holds for various K and h values (see Fig A.1 in).

Now, we discuss how much the relative diversity S^*/M^* can increase, considering its bounds. Utilizing the inequality of $0 \leq \gamma^{-1} \sigma_C^2 \nu \chi < 1/2$ (see details in Sec. A.4), we determine the lower and the upper bounds of S^*/M^* as

$$\gamma^{-1} h \nu \leq S^*/M^* < \gamma^{-1} h \nu + 1/2. \quad (3)$$

With the precise expressions of abundance distributions, we obtain the boundaries more thoroughly than before [25]. Without intraspecific suppression, S^*/M^* lies between 0 and $1/2$, and the CEP holds. With intraspecific suppression, however, the lower and the upper bounds increase by $\gamma^{-1} h \nu$, which is positive. Thus, it is possible for S^*/M^* to surpass the CEP bound for strong intraspecific suppression, and indeed it occurs as shown in Fig 2(a).

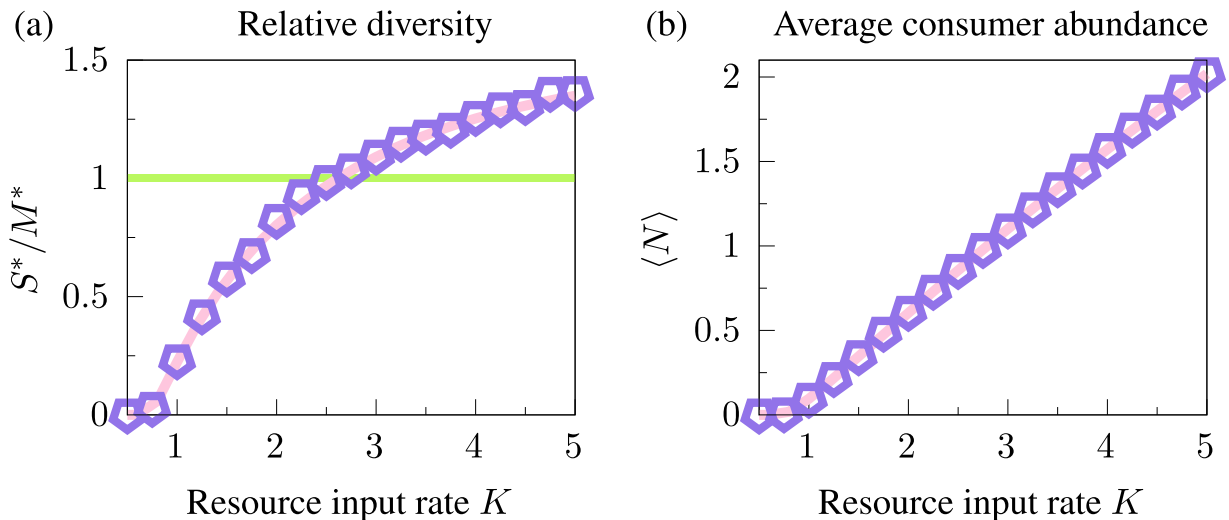


FIG. 4. (a) Relative diversity S^*/M^* and (b) average consumer abundance $\langle N \rangle$ against the resource input rate K for the fixed ratio $\gamma = M/S = 2/3$. The relative diversity exceeds the CEP bound only when the environment supplies the resource rich enough (large resource input rate). The effect of intraspecific suppression is amplified in rich environments because the consumers have higher pressure with larger abundances. We used the intraspecific suppression coefficient $h = 1/10$ and the deviation of consumption rate $\sigma_C = 1/10$.

Rich environment is essential to enhance biodiversity through intraspecific suppression

Environmental conditions play a crucial role in determining whether the relative diversity S^*/M^* surpasses the CEP bound. In a resource-rich environment (high K), the resources are abundant, and lots of consumers can access the resources and utilize them for their own survival. In comparison, in a resource-poor environment (low K), the resources are scarce, and most consumers cannot get the resources and die, not satisfying their minimum energy for survival. Therefore, the resource-rich environment is required to observe higher relative diversity, as shown in Fig 4. The relative diversity S^*/M^* can surpass 1 only when the resource is rich enough (see Fig 4(a), and Figs B.1–4 in). It means that intraspecific suppression has a high impact in a resource-rich environment (see five figures in left column of Fig B.4 in) while the effect is relatively negligible in a resource-poor environment (see five figures in right column of Fig B.4. in). It is because the consumers cannot grow well in resource-poor environments, i.e., one's abundance N_i is low, and thus the growth suppression by intraspecific suppression becomes weak as it is in the second order of N_i . As the large resource input amplifies the effect of intraspecific suppression, both an increase in the intraspecific suppression coefficient h and an increase in the resource input rate K enhance the relative diversity S^*/M^* as shown in Fig. 5 and Fig B.1 in . The results of S^*/M^* in (h, K) -plane for different σ_C , in (h, σ_C) -plane for different K , and in (σ_C, K) -plane for different h are exhibited in Figs B.1–3 in , respectively.

On the other hand, S^*/M^* exhibits nontrivial behavior with respect to σ_C . In the absence of intraspecific suppression, the augmentation of σ_C elevates S^*/M^* in both resource-rich and resource-poor environments (see Fig B.3(a) and Fig B.4(a)–(c) in), as predicted in the niche theory. Similar trends are observed with intraspecific suppression in resource poor environments where the impact of intraspecific suppression is minimal. However, in resource-rich environments, the increase in σ_C leads to a reduction in S^*/M^* under intraspecific suppression (see Fig B.3(b)–(f), and Fig B.4(a)–(c) in). This nontrivial behavior in resource-rich environments can be understood by examining the effective consumer growth rate g_{eff} and the deviation in consumer growth rate σ_g . The pivotal factor lies in the sign of g_{eff} . When resources are abundant, g_{eff} has a positive value with intraspecific suppression, indicating that the species can typically meet their minimum energy demand ($g_{\text{eff}} > 0$), while without intraspecific suppression, g_{eff} has negative value (see Fig B.4(d)–(f) in). Consequently, the increased σ_g resulting from elevated σ_C elicits the opposite effect on relative diversity (see Fig B.4(g)–(i) in). In summary, the effect of σ_C on S^*/M^* is determined by the other parameters such as K and h , while increases in K and h consistently enhance the biodiversity as shown in Fig. 5.

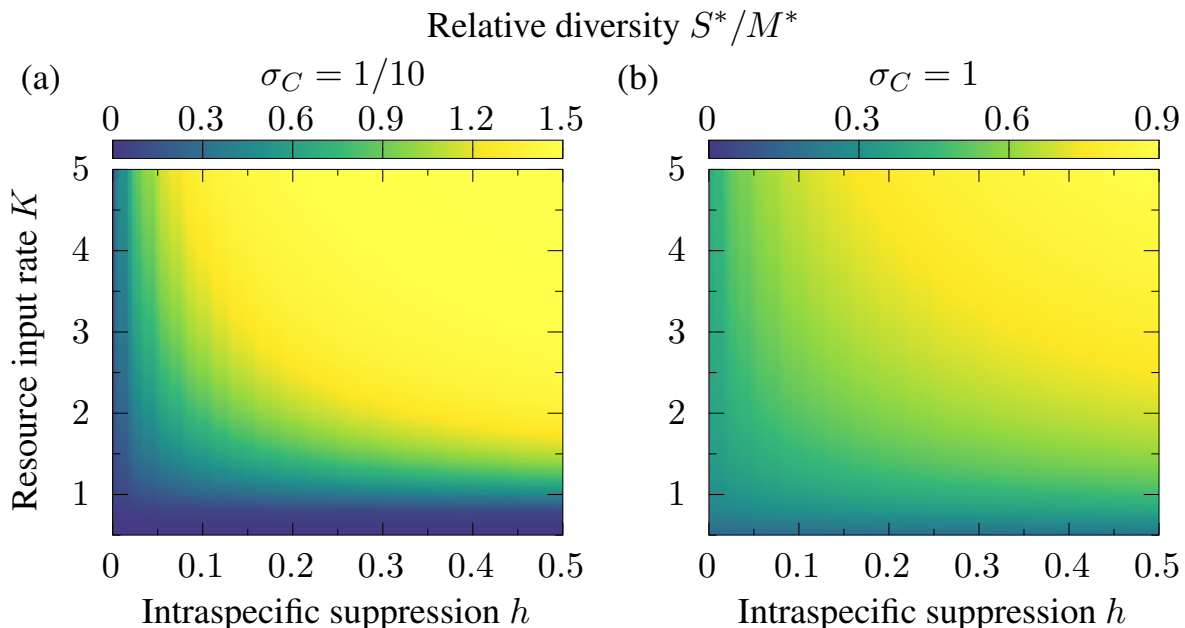


FIG. 5. Relative diversity S^*/M^* in (h, K) -plane for (a) $\sigma_C = 1/10$ and (b) $\sigma_C = 1$. In resource-poor environments, characterized by small values of K , the relative diversity cannot surpass the CEP bound of 1, even with intraspecific suppression. However, as K increases, the relative diversity S^*/M^* can surpass the CEP bound with intraspecific suppression. In the absence of intraspecific suppression ($h = 0$), even in resource-rich environments, the relative diversity S^*/M^* remains below $1/2$, which is the upper bound found in the previous study [25]. This suggests that intraspecific suppression and resource-rich environments are necessary conditions to achieve relative diversity beyond the CEP bound.

CONCLUSION AND DISCUSSIONS

In this paper, we have investigated the effect of intraspecific suppression on consumer diversity in large ecological systems. Employing the cavity method and generating functional analysis, we derived the consumer abundance distribution $P(N)$, the resource abundance distribution $P(R)$, formula of the relative diversity S^*/M^* , and its lower and upper bounds. Our theoretical findings have been validated through comparison with numerical simulation results. Notably, our results demonstrate that intraspecific suppression serves to augment consumer diversity and has the potential to increase the number of coexisting consumers beyond the available resources. This observation helps to elucidate the plankton paradox within competition-based models.

Intraspecific suppression has already been considered in many ecological systems [17, 22, 44, 45], showing an important role in the stability of the coexistence of consumer and resource species. However, such studies have focused on two [44] or three [45] species representing each trophic level rather than how many consumer species can survive with respect to the available resource kinds. Even though it is well known that intraspecific suppression can stabilize the coexistence between a resource and a consumer species, the extension of intraspecific suppression's role in fostering diversity beyond the CEP within large ecosystems containing a large number of different species and resources is a non-trivial endeavor. By integrating intraspecific suppression into GCRM, we have demonstrated intraspecific suppression has the capability to augment biodiversity beyond the constraints of the CEP, particularly in resource-rich environments. This enhancement occurs through the suppression of dominant species emergence.

In previous studies on GCRM [25, 27], the parameter σ_C , representing the deviation in consumption rates, has been considered to control niche overlap. When σ_C is zero, all species consume resources at identical rates, leading to complete niche overlap. Conversely, higher values of σ_C result in diverse consumption rates among species, thereby reducing niche overlap. According to the niche theory, species can coexist by reducing the niche overlap, hence increasing σ_C can enlarge biodiversity. This interpretation explains the increasing relative diversity S^*/M^* in σ_C in the absence of intraspecific suppression. However, with intraspecific suppression, this interpretation encounters challenges. In resource-rich environments, biodiversity decreases as σ_C increases. This phenomenon arises because the upper bound on consumer diversity within the CEP is influenced by all constraining factors, including available

resources. Introducing intraspecific suppression implicitly introduces an additional limiting factor, necessitating the consideration of both σ_C and h in defining the niche. While intraspecific suppression can act as a limiting factor, its impact varies with environmental conditions, as observed in our findings. This underscores the notion that the interpretation of niche dynamics should be contingent upon the specific details of the ecological system.

We have utilized consumer and resource abundance statistics, focusing solely on the interactions between two trophic levels. Our methodology is adaptable to ecological systems featuring trophic structures comprising more than two levels. For instance, we can extend the system to encompass ecosystems with three or more trophic levels, incorporating predator species, intermediate species preyed upon by predators while consuming prey species, and externally supplied prey species. In this extension, predation would conceivably play an important role in biodiversity, serving as a limiting factor [13]. Furthermore, our approach could provide valuable insights into comprehending the dynamics of broader ecological systems characterized by structural complexity.

METHODS

For simulations, we numerically integrate Eq. (1) for 50 independent realizations of the model parameters with random initial conditions using the Runge-Kutta-Fehlberg (RKF) method [46]. For each realization, we use $S = 75$ consumers and $M = 50$ resources. The RKF method changes the step size Δt adaptively by comparing the integration results in the order of $\mathcal{O}(\Delta t^4)$ and $\mathcal{O}(\Delta t^5)$. In the numerical integration, we regard a species goes extinct when its abundance has lower value than the extinction threshold 10^{-9} .

We also obtain the solutions of self-consistent equations using the optimization method, Nelder-Mead algorithm [47]. Our optimization function is designed as the sum of differences between the given values of seven macroscopic quantities, namely ϕ_S , $\langle N \rangle$, $\langle N^2 \rangle$, ν , $\langle R \rangle$, $\langle R^2 \rangle$, and χ , and the corresponding values obtained by integrating the abundance distributions $P(N)$ and $P(R)$, as described in Eq. (A.26) in . The algorithm aims to minimize this optimization function by seeking appropriate values for the quantities. We set the tolerance parameter for the optimization to 10^{-31} .

SUPPORTING INFORMATION

S1 Appendix. **Section A.** Derivations of consumer and resource abundance distributions using cavity method and generating functional analysis. **Section B.** Numerical simulation results. **Section C.** Results for self-renewing resources. **Section D.** Extension to three-trophic level systems. (PDF)

ACKNOWLEDGMENTS

The authors acknowledge Deok-Sun Lee, Hyeong-Chai Jeong, and Jong Il Park for fruitful discussion. This work was supported by a KIAS individual Grant CG091401 at Korea Institute for Advanced Study (S.-G.Y.), an appointment to the YST Program at the APCTP through the Science and Technology Promotion Fund and Lottery Fund of the Korean Government, as well as by the Korean Local Governments — Gyeongsangbuk-do Province, and Pohang City (S.-G.Y.), and the National Research Foundation of Korea grant funded by the Korea government (MSIT), Grant No. RS-2023-00214071 (H.J.P.). This work was supported by INHA UNIVERSITY Research Grant as well (H.J.P.).

-
- [1] J. H. Vandermeer, Niche theory, *Annu. Rev. Ecol. Syst.* **3**, 107 (1972).
 - [2] G. Hardin, The competitive exclusion principle, *Science* **131**, 3409 (1960).
 - [3] G. F. Gause, Experimental analysis of Vito Volterra's mathematical theory of the struggle for existence, *Science* **79**, 16 (1934).
 - [4] G. F. Gause, *The Struggle for Existence: A Classic of Mathematical Biology and Ecology* (The Williams & Wilkins company, 1934).
 - [5] R. H. MacArthur, Population ecology of some warblers of northeastern coniferous forests, *Ecology* **39**, 599 (1958).
 - [6] R. H. MacArthur and R. Levins, The limiting similarity, convergence, and divergence of coexisting species, *Am. Nat.* **101**, 377 (1967).
 - [7] S. A. Levin, Community equilibria and stability, and an extension of the competitive exclusion principle, *Am. Nat.* **104**, 413 (1970).

- [8] R. McGehee and R. A. Armstrong, Some mathematical problems concerning the ecological principle of competitive exclusion, *J. Differ. Equations* **23**, 30 (1977).
- [9] G. E. Hutchinson, The paradox of the plankton, *Am. Nat.* **95**, 127 (1961).
- [10] A. Sournia, M.-J. Chrétiennot-Dinet, and M. Ricard, Marine phytoplankton: how many species in the world ocean?, *J. Plankton Res.* **13**, 1093 (1991).
- [11] P. Tett and E. D. Barton, Why are there about 5000 species of phytoplankton in the sea?, *J. Plankton Res.* **17**, 1693 (1995).
- [12] C. De Vargas, S. Audic, N. Henry, J. Decelle, F. Mahé, R. Logares, E. Lara, C. Berney, N. Le Bescot, I. Probert, *et al.*, Eukaryotic plankton diversity in the sunlit ocean, *Science* **348**, 1261605 (2015).
- [13] S. Roy and J. Chattopadhyay, Towards a resolution of ‘the paradox of the plankton’: A brief overview of the proposed mechanisms, *Ecol. Complex.* **4**, 26 (2007).
- [14] D. Gupta, S. Garlaschi, S. Suweis, S. Azaele, and A. Maritan, Effective resource competition model for species coexistence, *Phys. Rev. Lett.* **127**, 208101 (2021).
- [15] G. Barabás, M. J. Michalska-Smith, and S. Allesina, Self-regulation and the stability of large ecological networks, *Nat. Ecol. Evol.* **1**, 1870 (2017).
- [16] C. Picoche and F. Barraquand, Strong self-regulation and widespread facilitative interactions in phytoplankton communities, *J. Ecol.* **108**, 2232 (2020).
- [17] P. Chesson, Mechanisms of maintenance of species diversity, *Annu. Rev. Ecol. Syst.* **31**, 343 (2000).
- [18] F. Rodriguez-Valera, A.-B. Martín-Cuadrado, B. Rodriguez-Brito, L. Pasic, T. F. Thingstad, F. Rohwer, and A. Mira, Explaining microbial population genomics through phage predation, *Nat. Preced.* <https://doi.org/10.1038/npre.2009.3489.1> (2009).
- [19] T. F. Thingstad, Elements of a theory for the mechanisms controlling abundance, diversity, and biogeochemical role of lytic bacterial viruses in aquatic systems, *Linnol. Oceanogr.* **45**, 1320 (2020).
- [20] S. Maslov and K. Sneppen, Maximal feeding with active prey-switching: A kill-the-winner functional response and its effect on global diversity and biogeography, *Sci. Rep.* **7**, 39642 (2017).
- [21] S. M. Vallina, B. A. Ward, S. Dutkiewicz, and M. J. Follows, Maximal feeding with active prey-switching: A kill-the-winner functional response and its effect on global diversity and biogeography, *Prog. Oceanogr.* **120**, 93 (2014).
- [22] R. H. MacArthur, Species packing and competitive equilibrium for many species, *Theor. Popul. Biol.* **1**, 1 (1970).
- [23] R. H. MacArthur, Species packing, and what interspecies competition minimizes, *Proc. Natl. Acad. Sci. USA* **64**, 1369 (1969).
- [24] P. Chesson, MacArthur’s consumer-resource model, *Theor. Popul. Biol.* **37**, 26 (1990).
- [25] W. Cui, R. Marsland III, and P. Mehta, Effect of resource dynamics on species packing in diverse ecosystems, *Phys. Rev. Lett.* **125**, 048101 (2020).
- [26] R. M. May, Will a large complex system be stable?, *Nature* **238**, 413 (1972).
- [27] M. Advani, G. Bunin, and P. Mehta, Statistical physics of community ecology: a cavity solution to MacArthur’s consumer resource model, *J. Stat. Mech.* , 033406 (2018).
- [28] A. R. Batista-Tomás, A. D. Martino, and R. Mulet, Path-integral solution of MacArthur’s resource-competition model for large ecosystems with random species-resources couplings, *Chaos* **31**, 103113 (2021).
- [29] S. Allesina and S. Tang, Stability criteria for complex ecosystems, *Nature* **483**, 205 (2012).
- [30] I. Dalmedigos and G. Bunin, Dynamical persistence in high-diversity resource-consumer communities, *PLOS Comput. Biol.* **16**, e1008189 (2020).
- [31] G. Bunin, Ecological communities with Lotka-Volterra dynamics, *Phys. Rev. E* **95**, 042414 (2017).
- [32] M. Barbier and J.-F. Arnoldi, The cavity method for community ecology, *bioRxiv*: 147728 (2017).
- [33] T. Galla, Dynamically evolved community size and stability of random Lotka-Volterra ecosystems, *Europhys. Lett.* **123**, 48004 (2018).
- [34] J. W. Baron, T. J. Jewell, C. Ryder, and T. Galla, Eigenvalues of random matrices with generalized correlations: A path integral approach, *Phys. Rev. Lett.* **128**, 120601 (2022).
- [35] J. W. Baron, T. J. Jewell, C. Ryder, and T. Galla, Breakdown of random-matrix universality in persistent Lotka-Volterra communities, *Phys. Rev. Lett.* **130**, 137401 (2023).
- [36] M. Mézard, G. Parisi, and M. A. Virasoro, *Spin Glass Theory and Beyond: An Introduction to the Replica Method and Its Applications*, Vol. 9 (World Scientific, Singapore, 1987).
- [37] M. Mézard and G. Parisi, The Bethe lattice spin glass revisited, *Eur. Phys. J. B* **20**, 217 (2001).
- [38] F. Krzakala, F. Ricci-Tersenghi, L. Zdeborova, E. W. Tramel, R. Zecchina, and L. F. Cugliandolo, *Statistical Physics, Optimization, Inference, and Message-Passing Algorithms: Lecture Notes of the Les Houches School of Physics: Special Issue, October 2013*, 2013 (Oxford University Press, 2016).
- [39] C. De Dominicis, Dynamics as a substitute for replicas in systems with quenched random impurities, *Phys. Rev. B* **18**, 4913 (1978).
- [40] C. De Dominicis and I. Giardina, *Random Fields and Spin Glasses: A Field Theory Approach* (Cambridge University Press, 2006).
- [41] M. Helias and D. Dahmen, *Statistical Field Theory for Neural Networks*, Vol. 970 (Springer, Berlin, 2020).
- [42] A. Coolen, Statistical Mechanics of Recurrent Neural Networks II – Dynamics, in *Neuro-Informatics and Neural Modelling*, Handbook of Biological Physics, Vol. 4, edited by F. Moss and S. Gielen (North-Holland, 2001) pp. 619–684.
- [43] A. Altieri, G. Biroli, and C. Cammarota, Dynamical mean-field theory and aging dynamics, *J. Phys. A: Math. Theor.* **53**, 375006 (2020).

- [44] Yusrianto, S. Toaha, and Kasbawati, Stability analysis of prey predator model with holling ii functional response and threshold harvesting for the predator, *J. Phys.: Conf. Ser.* **1341**, 062025 (2019).
- [45] N. Ali, M. Haque, E. Venturino, and S. Chakravarty, Dynamics of a three species ratio-dependent food chain model with intra-specific competition within the top predator, *Comput. Biol. Med.* **85**, 63 (2017).
- [46] W. H. Press, S. A. Teukolsky, W. T. Vetterling, and B. P. Flannery, *Numerical Recipes: The Art of Scientific Computing*, 3rd ed. (New York: Cambridge Univ. Press, 2007).
- [47] J. A. Nelder and R. Mead, A simplex method for function minimization, *Comput. J.* **7**, 308 (1965).

Appendix: Enhancing biodiversity through intraspecific suppression in large ecosystems

Seong-Gyu Yang (양성규)^{1,2} and Hye Jin Park (박혜진)^{3,*}

¹*School of Computational Sciences, Korea Institute for Advanced Study, Seoul, 02455, Republic of Korea*

²*Asia Pacific Center for Theoretical Physics, Pohang, 37673, Republic of Korea*

³*Department of Physics, Inha University, Incheon 22212, Republic of Korea*

(Dated: April 2, 2024)

CONTENTS

A. Derivations	1
A.1. Cavity method	1
A.2. Generating functional analysis	2
A.3. Abundance distributions	8
A.4. Bounds of the relative diversity	10
B. Numerical simulation results	11
C. Self-renewing resources	23
D. Three-trophic level systems	29
References	29

A. DERIVATIONS

A.1. Cavity method

In this section, we derive cavity solutions of consumer and resource abundances, following the similar process in Ref. [1–3]. The consumption rate $C_{i\alpha}$ in

$$\begin{aligned}\dot{N}_i &= N_i \left(\sum_{\alpha} C_{i\alpha} R_{\alpha} - m_i - h_i N_i \right), \\ \dot{R}_{\alpha} &= K_{\alpha} - \left(D_{\alpha} + \sum_i N_i C_{i\alpha} \right) R_{\alpha},\end{aligned}\tag{A.1}$$

has quenched disorder as $C_{i\alpha} = \mu_C/M + z_{i\alpha}^C \sigma_C/\sqrt{M}$, where $z_{i\alpha}^C$ is an independent unit Gaussian random variable. Other parameters including mortality rate $m_i = m + z_i^m \sigma_m$, intraspecific suppression coefficient $h_i = h + z_i^h \sigma_h$, resource input rate $K_{\alpha} = K + z_{\alpha}^K \sigma_K$, and degradation rate $D_{\alpha} = D + z_{\alpha}^D \sigma_D$ also have quenched disorder, where $z_i^m, z_i^h, z_{\alpha}^K$, and z_{α}^D are unit Gaussian random variables. Separating the parameters into mean and deviation parts, Eq. (A.1) can be rewritten as follows:

$$\begin{aligned}\dot{N}_i &= N_i \left(\mu_C \langle R \rangle - m - h N_i - z_i^m \sigma_m - z_i^h \sigma_h N_i + \frac{\sigma_C}{\sqrt{M}} \sum_{\alpha} z_{i\alpha}^C R_{\alpha} \right), \\ \dot{R}_{\alpha} &= K + z_{\alpha}^K \sigma_K - \left(D + \gamma^{-1} \mu_C \langle R \rangle + z_{\alpha}^D \sigma_D + \frac{\sigma_C}{\sqrt{M}} \sum_i z_{i\alpha}^C N_i \right) R_{\alpha},\end{aligned}\tag{A.2}$$

* hyejin.park@inha.ac.kr

where $\gamma \equiv M/S$ is the number ratio between consumers and resources, and $\langle N \rangle$ and $\langle R \rangle$ denote the average consumer abundance and average resource abundance, respectively.

We consider the immigration of a cavity consumer ($i = 0$), and an additional supply of a cavity resource ($\alpha = 0$) into a system, assuming that the cavity species and the cavity resource follow the same rule as others. Those cavities act like small perturbations on the system. The cavity consumer perturbs the degradation rate as $dD_\alpha = \frac{\sigma_C}{\sqrt{M}} N_0 z_{0\alpha}^C$ and the cavity resource perturbs the consumer's mortality rate as $dm_i = -\frac{\sigma_C}{\sqrt{M}} R_0 z_{i0}^C$. Under those perturbations, we assume that the system linearly responds to those perturbations as

$$\begin{aligned} N_i &\approx N_{i\setminus 0} + \sum_{j\setminus 0} \frac{\partial N_i}{\partial m_j} dm_j + \sum_{\beta\setminus 0} \frac{\partial N_i}{\partial D_\beta} dD_\beta \\ &= N_{i\setminus 0} + \frac{\sigma_C}{\sqrt{M}} R_0 \sum_{j\setminus 0} z_{j0}^C \nu_{ij}^N - \frac{\sigma_C}{\sqrt{M}} N_0 \sum_{\beta\setminus 0} z_{0\beta}^C \chi_{i\beta}^N, \\ R_\alpha &\approx R_{\alpha\setminus 0} + \sum_{k\setminus 0} \frac{\partial R_\alpha}{\partial m_k} dm_k + \sum_{\lambda\setminus 0} \frac{\partial R_\alpha}{\partial D_\lambda} dD_\lambda \\ &= R_{\alpha\setminus 0} + \frac{\sigma_C}{\sqrt{M}} R_0 \sum_{k\setminus 0} z_{k0}^C \nu_{\alpha k}^R - \frac{\sigma_C}{\sqrt{M}} N_0 \sum_{\lambda\setminus 0} z_{0\lambda}^C \chi_{\alpha\lambda}^R, \end{aligned} \quad (\text{A.3})$$

where $\nu_{ij}^N \equiv -\partial N_i / \partial m_j$, $\nu_{\alpha i}^R \equiv -\partial R_\alpha / \partial m_i$, $\chi_{i\alpha}^N \equiv -\partial N_i / \partial D_\alpha$, and $\chi_{\alpha\beta}^R \equiv -\partial R_\alpha / \partial D_\beta$ are response functions for the perturbations. To calculate the feedback to the response, we insert Eq. (A.3) into the equations of motion of cavities. Since we are dealing with the large ecosystem ($S \rightarrow \infty$, $M \rightarrow \infty$), those perturbations from cavities are assumed to not change all macroscopic quantities. Thus, the equation for cavity consumer and cavity resource can be rewritten as follows:

$$\begin{aligned} \dot{N}_0 &= N_0 \left[\mu_C \langle R \rangle - m - h N_0 - z_0^m \sigma_m - z_0^h \sigma_h N_0 + \frac{\sigma_C}{\sqrt{M}} z_{00}^C R_0 \right. \\ &\quad \left. + \frac{\sigma_C}{\sqrt{M}} \sum_{\alpha\setminus 0} z_{0\alpha}^C \left(R_{\alpha\setminus 0} - \frac{\sigma_C}{\sqrt{M}} N_0 \sum_{\lambda\setminus 0} z_{0\lambda}^C \chi_{\alpha\lambda}^R + \frac{\sigma_C}{\sqrt{M}} R_0 \sum_{k\setminus 0} z_{k0}^C \nu_{\alpha k}^R \right) \right], \\ \dot{R}_0 &= K + z_0^K \sigma_K - \left[D + \gamma^{-1} \mu_C \langle R \rangle + z_0^D \sigma_D + \frac{\sigma_C}{\sqrt{M}} z_{00}^C N_0 \right. \\ &\quad \left. + \frac{\sigma_C}{\sqrt{M}} \sum_{i\setminus 0} z_{i0}^C \left(N_{i\setminus 0} + \frac{\sigma_C}{\sqrt{M}} R_0 \sum_{j\setminus 0} z_{j0}^C \nu_{ij}^N - \frac{\sigma_C}{\sqrt{M}} N_0 \sum_{\beta\setminus 0} z_{0\beta}^C \chi_{i\beta}^N \right) \right] R_0. \end{aligned} \quad (\text{A.4})$$

Utilizing the property of independent random variables, the last terms in Eq. (A.4) go to zero. Ignoring those terms, we get the equations that cavity consumer and resource should follow at a steady state,

$$\begin{aligned} 0 &= N \left[\mu_C \langle R \rangle - m - (h + \sigma_C^2 \chi) N + z_N \sqrt{\sigma_m^2 + \sigma_h^2 N^2 + \sigma_C^2 \langle R^2 \rangle} \right], \\ 0 &= -\gamma^{-1} \sigma_C^2 \nu R^2 - (D + \gamma^{-1} \mu_C \langle R \rangle) R + K + z_R \sqrt{\sigma_K^2 + (\sigma_D^2 + \gamma^{-1} \sigma_C^2 \langle N^2 \rangle) R^2}, \end{aligned} \quad (\text{A.5})$$

where $\nu \equiv \frac{1}{S} \sum_i \nu_{ii}^N$ and $\chi \equiv \frac{1}{M} \sum_\alpha \chi_{\alpha\alpha}^R$, and z_N and z_R are independent unit Gaussian random variables. Since all species behave in the same way as the cavity species, we omit the subscript 0 in Eq. (A.5).

A.2. Generating functional analysis

We now obtain the same result of Eq. (A.5) using generating functional analysis, following the similar procedure described in Ref. [4, 5]. The generating functional can be written as follows:

$$Z(\psi, \phi) = \left\langle \exp \left(i \sum_j \int dt \psi_j(t) N_j(t) + i \sum_\alpha \int dt \phi_\alpha(t) R_\alpha(t) \right) \right\rangle, \quad (\text{A.6})$$

where ψ , and ϕ are auxiliary fields. Here, $\langle \dots \rangle$ and $\overline{\dots}$ denote the path and the disorder averages, respectively. Inside Eq. (A.6), $N_j(t)$ and $R_\alpha(t)$ should follow Eq. (A.1). We apply the time-dependent response probing fields in Eq. (A.1), and the path average is written as

$$\begin{aligned}
Z(\psi, \phi) &= \overline{\int \mathcal{D}[N] \mathcal{D}[\mathbf{R}] \exp\left(i \sum_j \int dt \psi_j N_j\right) \exp\left(i \sum_\alpha \int dt \phi_\alpha R_\alpha\right)} \\
&\times \overline{\prod_{t,j} \delta\left[\frac{\dot{N}_j}{N_j} - \sum_\alpha C_{j\alpha} R_\alpha + m_j + \eta_j^m + (h_j + \eta_j^h) N_j\right]} \\
&\times \overline{\prod_{t,\alpha} \delta\left(\frac{\dot{R}_\alpha - K_\alpha - \eta_\alpha^K}{R_\alpha} + D_\alpha + \eta_\alpha^D + \sum_j C_{j\alpha} N_j\right)},
\end{aligned} \tag{A.7}$$

where $\eta^m(t)$, $\eta^h(t)$, $\eta^D(t)$, and $\eta^K(t)$ are the response probing fields. Utilizing the property of the delta function and separating it into mean and disorder parts, we rewrite Eq. (A.7) as

$$\begin{aligned}
Z(\psi, \phi) &= \int \mathcal{D}[N, \hat{N}] \mathcal{D}[\mathbf{R}, \hat{\mathbf{R}}] \exp\left(i \sum_j \int dt \psi_j N_j\right) \exp\left(i \sum_\alpha \int dt \phi_\alpha R_\alpha\right) \\
&\times \exp\left[i \sum_j \int dt \hat{N}_j \left(\frac{\dot{N}_j}{N_j} - \frac{\mu_C}{M} \sum_\alpha R_\alpha + m_j + \eta_j^m + (h_j + \eta_j^h) N_j\right)\right] \\
&\times \exp\left[i \sum_\alpha \int dt \hat{R}_\alpha \left(\frac{\dot{R}_\alpha - K_\alpha - \eta_\alpha^K}{R_\alpha} + D_\alpha + \eta_\alpha^D + \gamma \frac{\mu_C}{S} \sum_j N_j\right)\right] \\
&\times \exp\left[i \sum_j \int dt \hat{N}_j \left(-\frac{\sigma_C}{\sqrt{M}} \sum_\alpha R_\alpha z_{j\alpha}^C + \sigma_m z_j^m + \sigma_h z_j^h N_j\right)\right] \\
&\times \exp\left[i \sum_\alpha \int dt \hat{R}_\alpha \left(\frac{\sigma_C}{\sqrt{M}} \sum_j N_j z_{j\alpha}^C + \sigma_D z_\alpha^D - \frac{\sigma_K}{R_\alpha} z_\alpha^K\right)\right],
\end{aligned} \tag{A.8}$$

where z^C , z^m , z^h , z^D , and z^K are unit Gaussian random variables. Then, we do not need to take the disorder average for all terms but only for the terms with disorders. After averaging over disorder utilizing the cumulant expansion for

the Gaussian random variables, we obtain the generating functional as

$$\begin{aligned}
Z(\psi, \phi) &= \int \mathcal{D}[N, \hat{N}] \mathcal{D}[\mathbf{R}, \hat{\mathbf{R}}] \exp \left(i \sum_j \int dt \psi_j N_j \right) \exp \left(i \sum_\alpha \int dt \phi_\alpha R_\alpha \right) \\
&\times \exp \left[i \sum_j \int dt \hat{N}_j \left(\frac{\dot{N}_j}{N_j} - \frac{\mu_C}{M} \sum_\alpha R_\alpha + m_j + \eta_j^m + (h_j + \eta_j^h) N_j \right) \right] \\
&\times \exp \left[i \sum_\alpha \int dt \hat{R}_\alpha \left(\frac{\dot{R}_\alpha - K_\alpha - \eta_\alpha^K}{R_\alpha} + D_\alpha + \eta_\alpha^D + \gamma \frac{\mu_C}{S} \sum_j N_j \right) \right] \\
&\times \exp \left[-\frac{\sigma_m^2}{2} \sum_j \iint dt dt' \hat{N}_j \hat{N}'_j \right] \\
&\times \exp \left[-\frac{\sigma_h^2}{2} \sum_j \iint dt dt' N_j \hat{N}_j N'_j \hat{N}'_j \right] \\
&\times \exp \left[-\frac{\sigma_K^2}{2} \sum_\alpha \iint dt dt' \frac{\hat{R}_\alpha \hat{R}'_\alpha}{R_\alpha R'_\alpha} \right] \\
&\times \exp \left[-\frac{\sigma_C^2}{2M} \sum_{j,\alpha} \iint dt dt' \left(N_j N'_j \hat{R}_\alpha \hat{R}'_\alpha + \hat{N}_j \hat{N}'_j R_\alpha R'_\alpha - 2N_j \hat{N}'_j R'_\alpha \hat{R}_\alpha \right) \right], \tag{A.9}
\end{aligned}$$

where the variables $X \equiv X(t)$, and $X' \equiv X(t')$. From Eq. (A.9), we obtain macroscopic quantities by derivative with field variables

$$\begin{aligned}
\rho_N(t) &\equiv \frac{1}{S} \sum_j N_j(t) = -i \frac{1}{S} \sum_j \lim_{\varphi \rightarrow 0} \frac{\partial Z(\varphi)}{\partial \psi_j(t)}, \\
\rho_R(t) &\equiv \frac{1}{M} \sum_\alpha R_\alpha(t) = -i \frac{1}{M} \sum_\alpha \lim_{\varphi \rightarrow 0} \frac{\partial Z(\varphi)}{\partial \phi_\alpha(t)}, \\
\lambda_N(t) &\equiv \frac{1}{S} \sum_j \hat{N}_j(t) = -i \frac{1}{S} \sum_j \lim_{\varphi \rightarrow 0} \frac{\partial Z(\varphi)}{\partial \eta_j^m(t)}, \\
\lambda_R(t) &\equiv \frac{1}{M} \sum_\alpha \hat{R}_\alpha(t) = -i \frac{1}{M} \sum_\alpha \lim_{\varphi \rightarrow 0} \frac{\partial Z(\varphi)}{\partial \eta_\alpha^D(t)}, \\
C_N(t, t') &\equiv \frac{1}{S} \sum_j N_j(t) N_j(t') = -\frac{1}{S} \sum_j \lim_{\varphi \rightarrow 0} \frac{\partial^2 Z(\varphi)}{\partial \psi_j(t) \partial \psi_j(t')}, \\
C_R(t, t') &\equiv \frac{1}{M} \sum_\alpha R_\alpha(t) R_\alpha(t') = -\frac{1}{M} \sum_\alpha \lim_{\varphi \rightarrow 0} \frac{\partial^2 Z(\varphi)}{\partial \phi_\alpha(t) \partial \phi_\alpha(t')}, \\
L_N(t, t') &\equiv \frac{1}{S} \sum_j \hat{N}_j(t) \hat{N}_j(t') = -\frac{1}{S} \sum_j \lim_{\varphi \rightarrow 0} \frac{\partial^2 Z(\varphi)}{\partial \eta_j^m(t) \partial \eta_j^m(t')}, \\
L_R(t, t') &\equiv \frac{1}{M} \sum_\alpha \hat{R}_\alpha(t) \hat{R}_\alpha(t') = -\frac{1}{M} \sum_\alpha \lim_{\varphi \rightarrow 0} \frac{\partial^2 Z(\varphi)}{\partial \eta_\alpha^D(t) \partial \eta_\alpha^D(t')}, \\
K_N(t, t') &\equiv \frac{1}{S} \sum_j N_j(t) \hat{N}_j(t') = -\frac{1}{S} \sum_j \lim_{\varphi \rightarrow 0} \frac{\partial^2 Z(\varphi)}{\partial \psi_j(t) \partial \eta_j^m(t')}, \\
K_R(t, t') &\equiv \frac{1}{M} \sum_\alpha R_\alpha(t) \hat{R}_\alpha(t') = -\frac{1}{M} \sum_\alpha \lim_{\varphi \rightarrow 0} \frac{\partial^2 Z(\varphi)}{\partial \phi_\alpha(t) \partial \eta_\alpha^D(t')}, \\
U_N(t, t') &\equiv \frac{1}{S} \sum_j N_j(t) N_j(t') \hat{N}_j(t) \hat{N}_j(t') = -\frac{1}{S} \sum_j \lim_{\varphi \rightarrow 0} \frac{\partial^2 Z(\varphi)}{\partial \eta_h^h(t) \partial \eta_j^h(t')}, \\
V_R(t, t') &\equiv \frac{1}{M} \sum_\alpha \frac{\hat{R}_\alpha(t) \hat{R}_\alpha(t')}{R_\alpha(t) R_\alpha(t')} = -\frac{1}{M} \sum_\alpha \lim_{\varphi \rightarrow 0} \frac{\partial^2 Z(\varphi)}{\partial \eta_\alpha^K(t) \partial \eta_\alpha^K(t')},
\end{aligned} \tag{A.10}$$

where $\varphi \equiv (\psi, \phi)$. We can easily find that $\lambda_N = \lambda_R = L_N = L_R = U_N = V_R = 0$, because $\lim_{\varphi \rightarrow 0} Z(\varphi) = 1$.

We define $\mathbf{\Pi} \equiv (\rho_N, \rho_R, \lambda_N, \lambda_R, C_N, C_R, L_N, L_R, K_N, K_R, U_N, V_R)$ to write the generating functional more shortly, and the generating functional is rewritten in terms of macroscopic quantities as follows:

$$Z(\varphi) = \int \mathcal{D}[\mathbf{\Pi}, \hat{\mathbf{\Pi}}] \exp \left[S \left(\Phi(\mathbf{\Pi}) + \Psi(\mathbf{\Pi}, \hat{\mathbf{\Pi}}) + \Omega_N(\hat{\mathbf{\Pi}}) + \Omega_R(\hat{\mathbf{\Pi}}) \right) \right], \tag{A.11}$$

where

$$\begin{aligned}
\Phi(\mathbf{\Pi}) &\equiv i\mu_C \int dt (\lambda_R \rho_N - \lambda_N \rho_R) \\
&\quad - \frac{\sigma_C^2}{2} \iint dt dt' [C_N(t, t') L_R(t, t') + L_N(t, t') C_R(t, t') - 2K_N(t, t') K_R(t, t')] \\
&\quad - \frac{1}{2} \iint dt dt' [\sigma_m^2 L_N(t, t') - \gamma \sigma_D^2 L_R(t, t') - \sigma_h^2 U_N(t, t') - \gamma \sigma_K^2 V_R(t, t')],
\end{aligned} \tag{A.12}$$

$$\begin{aligned}
\Psi(\mathbf{\Pi}, \hat{\mathbf{\Pi}}) &\equiv i \int dt \left(\hat{\rho}_N \rho_N + \hat{\lambda}_N \lambda_N + \gamma \hat{\rho}_R \rho_R + \gamma \hat{\lambda}_R \lambda_R \right) \\
&\quad + i \iint dt dt' \left[\hat{C}_N C_N + \hat{L}_N L_N + \hat{K}_N K_N + \hat{U}_N U_N \right] \\
&\quad + i \gamma \iint dt dt' \left[\hat{C}_R C_R + \hat{L}_R L_R + \hat{K}_R K_R + \hat{V}_R V_R \right],
\end{aligned} \tag{A.13}$$

$$\begin{aligned}
\Omega_N(\hat{\Pi}) \equiv & \frac{1}{S} \ln \left\{ \int \mathcal{D}[N, \hat{N}] \exp \left(i \sum_j \int dt \psi_j N_j \right) \right. \\
& \times \exp \left[i \sum_j \int dt \hat{N}_j \left(\frac{\dot{N}_j}{N_j} + m_j + h_j N_j + \eta_j^m + \eta_j^h N_j \right) \right. \\
& - i \int dt \left(\hat{\rho}_N \sum_j N_j + \hat{\lambda}_N \sum_j \hat{N}_j \right) - i \iint dt dt' \hat{U}_N \sum_j N_j N'_j \hat{N}_j \hat{N}'_j \\
& \left. \left. - i \iint dt dt' \left(\hat{C}_N \sum_j N_j N'_j + \hat{L}_N \sum_j \hat{N}_j \hat{N}'_j + \hat{K}_N \sum_j N_j \hat{N}'_j \right) \right] \right\}, \tag{A.14}
\end{aligned}$$

and

$$\begin{aligned}
\Omega_R(\hat{\Pi}) \equiv & \frac{1}{S} \ln \left\{ \int \mathcal{D}[\mathbf{R}, \hat{\mathbf{R}}] \exp \left(i \sum_\alpha \int dt \phi_\alpha R_\alpha \right) \right. \\
& \times \exp \left[i \sum_\alpha \int dt \hat{R}_\alpha \left(\frac{\dot{R}_\alpha - K_\alpha - \eta_\alpha^K}{R_\alpha} + D_\alpha + \eta_\alpha^D \right) \right. \\
& - i \int dt \left(\hat{\rho}_R \sum_\alpha R_\alpha + \hat{\lambda}_R \sum_\alpha \hat{R}_\alpha \right) - i \iint dt dt' \hat{V}_R \sum_\alpha \frac{\hat{R}_\alpha \hat{R}'_\alpha}{R_\alpha R'_\alpha} \\
& \left. \left. - i \iint dt dt' \left(\hat{C}_R \sum_\alpha R_\alpha R'_\alpha + \hat{L}_R \sum_\alpha \hat{R}_\alpha \hat{R}'_\alpha + \hat{K}_R \sum_\alpha R_\alpha \hat{R}'_\alpha \right) \right] \right\}. \tag{A.15}
\end{aligned}$$

Using the saddle-point approximation, we can evaluate Eq. (A.11) as $Z[\varphi] \approx \exp[S(\Phi^* + \Psi^* + \Omega_N^* + \Omega_R^*)]$, where Φ^* , Ψ^* , Ω_N^* , and Ω_R^* satisfy $\partial_{\Pi}(\Phi^* + \Psi^*) = 0$, and $\partial_{\hat{\Pi}}(\Psi^* + \Omega_N^* + \Omega_R^*) = 0$. From the first condition, we get the relations of

$$\begin{aligned}
\hat{\rho}_N &= \hat{\rho}_R = \hat{C}_N = \hat{C}_R = 0, \\
\hat{\lambda}_N &= \mu_C \rho_R, \\
\gamma \hat{\lambda}_R &= -\mu_C \rho_N, \\
i \hat{L}_N &= \frac{\sigma_C^2}{2} C_R + \frac{\sigma_m^2}{2}, \\
i \gamma \hat{L}_R &= \frac{\sigma_C^2}{2} C_N + \gamma \frac{\sigma_D^2}{2}, \\
i \hat{K}_N &= -\sigma_C^2 K_R(t, t'), \\
i \gamma \hat{K}_R &= -\sigma_C^2 K_N(t', t), \\
i \hat{U}_N &= \frac{\sigma_h^2}{2}, \\
i \hat{V}_R &= \frac{\sigma_K^2}{2}. \tag{A.16}
\end{aligned}$$

In addition, from the second condition, the macroscopic quantities are rewritten as

$$\begin{aligned}
\rho_N(t) &= \left\langle \frac{1}{S} \sum_i N_i(t) \right\rangle_{\star}, \\
\rho_R(t) &= \left\langle \frac{1}{M} \sum_{\alpha} R_{\alpha}(t) \right\rangle_{\star}, \\
\lambda_N(t) &= \left\langle \frac{1}{S} \sum_i \hat{N}_i(t) \right\rangle_{\star}, \\
\lambda_R(t) &= \left\langle \frac{1}{M} \sum_{\alpha} \hat{R}_{\alpha}(t) \right\rangle_{\star}, \\
C_N(t, t') &= \left\langle \frac{1}{S} \sum_i N_i(t) N_i(t') \right\rangle_{\star}, \\
C_R(t, t') &= \left\langle \frac{1}{M} \sum_{\alpha} R_{\alpha}(t) R_{\alpha}(t') \right\rangle_{\star}, \\
L_N(t, t') &= \left\langle \frac{1}{S} \sum_i \hat{N}_i(t) \hat{N}_i(t') \right\rangle_{\star}, \\
L_R(t, t') &= \left\langle \frac{1}{M} \sum_{\alpha} \hat{R}_{\alpha}(t) \hat{R}_{\alpha}(t') \right\rangle_{\star}, \\
K_N(t, t') &= \left\langle \frac{1}{S} \sum_i N_i(t) \hat{N}_i(t') \right\rangle_{\star}, \\
K_R(t, t') &= \left\langle \frac{1}{M} \sum_{\alpha} R_{\alpha}(t) \hat{R}_{\alpha}(t') \right\rangle_{\star}, \\
U_N(t, t') &= \left\langle \frac{1}{S} \sum_i N_i(t) N_i(t') \hat{N}_i(t) \hat{N}_i'(t') \right\rangle_{\star}, \\
V_R(t, t') &= \left\langle \frac{1}{M} \sum_{\alpha} \frac{\hat{R}_{\alpha}(t) \hat{R}_{\alpha}(t')}{R_{\alpha}(t) R_{\alpha}(t')} \right\rangle_{\star},
\end{aligned} \tag{A.17}$$

where $\langle A \rangle_{\star} \equiv \int \mathcal{D}[\mathbf{N}, \hat{\mathbf{N}}] \mathcal{D}[\mathbf{R}, \hat{\mathbf{R}}] A \exp(\dots) / \int \mathcal{D}[\mathbf{N}, \hat{\mathbf{N}}] \mathcal{D}[\mathbf{R}, \hat{\mathbf{R}}] \exp(\dots)$. Using the relations in Eq. (A.16) and the macroscopic quantities in Eq. (A.17), Ω_N^* and Ω_R^* are rewritten as follows:

$$\begin{aligned}
\Omega_N^* &= \ln \left\{ \int \mathcal{D}[\mathbf{N}, \hat{\mathbf{N}}] \exp \left(i \int dt \psi(t) N(t) \right) \right. \\
&\quad \times \exp \left[i \int dt \hat{N}(t) \left(\frac{\dot{N}(t)}{N(t)} - \mu_C \rho_R(t) + m + hN(t) \right. \right. \\
&\quad \quad \left. \left. - i\sigma_C^2 \int dt' K_R(t, t') N(t') + \eta^m(t) + \eta^h(t) N(t) \right) \right] \\
&\quad \left. \times \exp \left[-\frac{1}{2} \iint dt dt' \hat{N}(t) \hat{N}(t') (\sigma_C^2 C_R(t, t') + \sigma_m^2 + \sigma_h^2 N(t) N(t')) \right] \right\},
\end{aligned} \tag{A.18}$$

$$\begin{aligned}
\Omega_R^* = & \ln \left\{ \int \mathcal{D}[\mathbf{R}, \hat{\mathbf{R}}] \exp \left(i \int dt \phi(t) R(t) \right) \right. \\
& \times \exp \left[i \int dt \hat{R}(t) \left(\frac{\dot{R}(t) - K - \eta^K(t)}{R(t)} + D + \gamma^{-1} \mu_C \rho_N(t) \right. \right. \\
& \quad \left. \left. - i \gamma^{-1} \sigma_C^2 \int dt' K_N(t, t') R(t') + \eta^D(t) \right) \right] \\
& \left. \times \exp \left[-\frac{1}{2} \iint dt dt' \hat{R}(t) \hat{R}(t') \left(\gamma^{-1} \sigma_C^2 C_N(t, t') + \sigma_D^2 + \frac{\sigma_K^2}{R(t)R(t')} \right) \right] \right\}.
\end{aligned} \tag{A.19}$$

Now, we have the effective mean-field dynamics of consumer abundance from Eq. (A.18) and resource abundance from Eq. (A.19) as

$$\begin{aligned}
\dot{N}(t) = & N(t) \left[\mu_C \rho_R(t) - m(t) - h(t)N(t) \right. \\
& \left. + i \sigma_C^2 \int dt' K_R(t, t') N(t') - \eta^m(t) + \xi^N(t) - \eta^h(t)N(t) + \zeta^N(t)N(t) \right], \\
\dot{R}(t) = & K(t) + \eta^K(t) + \zeta^R(t) - \left[D(t) + \gamma^{-1} \mu_C \rho_N(t) \right. \\
& \left. - i \gamma^{-1} \sigma_C^2 \int dt' K_N(t, t') R(t') + \eta^D(t) + \xi^R(t) \right] R(t),
\end{aligned} \tag{A.20}$$

where $m(t) \equiv m + \eta^m(t)$, $h(t) \equiv h + \eta^h(t)$, $K(t) \equiv K + \eta^K(t)$, $D(t) \equiv D + \eta^D(t)$. Here, ξ^N and ξ^R are noises with $\langle \xi^N(t) \xi^N(t') \rangle = \sigma_C^2 C_R(t, t') + \sigma_m^2$ and $\langle \xi^R(t) \xi^R(t') \rangle = \gamma^{-1} \sigma_C^2 C_N(t, t') + \sigma_D^2$, and ζ^N and ζ^R are noises with $\langle \zeta^N(t) \zeta^N(t') \rangle = \sigma_h^2$ and $\langle \zeta^R(t) \zeta^R(t') \rangle = \sigma_K^2$. We rewrite the effective mean-field dynamics of Eq. (A.20) for zero response probing fields with defining $G_R(t, t') = -i K_R(t, t') = -\left\langle \frac{\partial R(t)}{\partial D(t')} \Big|_{D(t')=D} \right\rangle_\star$ and $G_N(t, t') = -i K_N(t, t') = -\left\langle \frac{\partial N(t)}{\partial m(t')} \Big|_{m(t')=m} \right\rangle_\star$ as

$$\begin{aligned}
\dot{N}(t) = & N(t) \left[\mu_C \rho_R(t) - m - hN(t) + \xi^N(t) + \zeta^N(t)N(t) - \sigma_C^2 \int dt' G_R(t, t') N(t') \right], \\
\dot{R}(t) = & K + \zeta^R(t) - \left[D + \gamma^{-1} \mu_C \rho_N(t) + \xi^R(t) + \gamma^{-1} \sigma_C^2 \int dt' G_N(t, t') R(t') \right] R(t).
\end{aligned} \tag{A.21}$$

At the steady state ($t \rightarrow \infty$), we assume that there are no long-term memories, then we can rewrite the response functions as functions of time difference as $G_X(t, t') = G_X(\tau)$ ($X = N, R$) where $\tau = t - t'$. In this state, the correlation functions become $C_N = \langle N^2 \rangle$, and $C_R = \langle R^2 \rangle$. We define the response functions as $\nu \equiv \int d\tau G_N(\tau)$ and $\chi \equiv \int d\tau G_R(\tau)$, and rewrite Eq. (A.21) as follows:

$$\begin{aligned}
0 = & N \left[\mu_C \rho_R - m - (h + \sigma_C^2 \chi) N + z_N \sqrt{\sigma_m^2 + \sigma_h^2 N^2 + \sigma_C^2 \langle R^2 \rangle} \right], \\
0 = & -\gamma^{-1} \sigma_C^2 \nu R^2 - (D + \gamma^{-1} \mu_C \rho_N) R + K + z_R \sqrt{\sigma_K^2 + (\sigma_D^2 + \gamma^{-1} \sigma_C^2 \langle N^2 \rangle) R^2},
\end{aligned} \tag{A.22}$$

where $z_N \sqrt{\sigma_m^2 + \sigma_h^2 N^2 + \sigma_C^2 \langle R^2 \rangle} = \xi^N + \zeta^N N$ and $z_R \sqrt{\sigma_K^2 + (\sigma_D^2 + \gamma^{-1} \sigma_C^2 \langle N^2 \rangle) R^2} = \zeta^R - \xi^R R$, and z_N and z_R are independent unit Gaussian random variables. The results are the same as the cavity solution of Eq. (A.5).

A.3. Abundance distributions

At the steady state, some consumers go extinct ($N = 0$) and the others survive with positive abundance $N = (g_{\text{eff}} + z_N \sqrt{\sigma_g^2 + \sigma_h^2 N^2}) / h_{\text{eff}}$, where $g_{\text{eff}} (\equiv \mu_C \rho_R - m)$ is the effective growth rate, $h_{\text{eff}} (\equiv h + \sigma_C^2 \chi)$ is the effective intraspecific suppression coefficient, and $\sigma_g^2 (\equiv \sigma_m^2 + \sigma_C^2 \langle R^2 \rangle)$ is the variance in the effective growth rate. The

resources have positive values for their abundance because the resources are supplied from outside with a constant input rate. To simplify the effective dynamics in Eq. (A.5) and Eq. (A.22), we define the effective degradation rate $D_{\text{eff}} (\equiv D + \gamma^{-1}\mu_C\langle N \rangle)$ and variance $\sigma_R^2 (\equiv \sigma_D^2 + \gamma^{-1}\sigma_C^2\langle N^2 \rangle)$ in effective degradation rate. Then, the abundances at the steady state in Eq. (A.5) and Eq. (A.22) are

$$\begin{aligned} z_N &= (h_{\text{eff}}N - g_{\text{eff}})/\sqrt{\sigma_g^2 + \sigma_h^2N^2} \quad \text{for } N > 0, \\ z_R &= (\gamma^{-1}\sigma_C^2\nu R^2 + D_{\text{eff}}R - K)/\sqrt{\sigma_R^2R^2 + \sigma_K^2}. \end{aligned} \quad (\text{A.23})$$

From Eq. (A.23), we obtain abundance distributions of consumer species $P(N)$ and resources $P(R)$ using the change of variables, i.e., $P(N) = P(z_N)|dz_N/dN|$ and $P(R) = P(z_R)|dz_R/dR|$, where $P(z) = \frac{1}{\sqrt{2\pi}}e^{-z^2/2}$. Here are the abundance distributions of consumer species and resources:

$$\begin{aligned} P(N) &= \frac{1}{\sqrt{2\pi}} \left| \frac{\sigma_h^2 g_{\text{eff}} N + \sigma_g^2 h_{\text{eff}}}{(\sigma_h^2 N^2 + \sigma_g^2)^{3/2}} \right| \exp \left[-\frac{(h_{\text{eff}}N - g_{\text{eff}})^2}{2(\sigma_h^2 N^2 + \sigma_g^2)} \right] \quad \text{for } N > 0, \\ P(R) &= \frac{1}{\sqrt{2\pi}} \frac{\gamma^{-1}\sigma_R^2\sigma_C^2\nu R^3 + (\sigma_R^2K + 2\gamma^{-1}\sigma_K^2\sigma_C^2\nu)R + \sigma_K^2D_{\text{eff}}}{(\sigma_R^2R^2 + \sigma_K^2)^{3/2}} \\ &\quad \times \exp \left[-\frac{(\gamma^{-1}\sigma_C^2\nu R^2 + D_{\text{eff}}R - K)^2}{2(\sigma_R^2R^2 + \sigma_K^2)} \right]. \end{aligned} \quad (\text{A.24})$$

Taking derivative on Eq. (A.22) and using the relation in Eq. (A.23), we obtain the response functions,

$$\begin{aligned} \nu(N) &= -\frac{\partial N}{\partial m} = \frac{\sigma_h^2 N^2 + \sigma_g^2}{h_{\text{eff}}\sigma_g^2 + \sigma_h^2 g_{\text{eff}}N}, \\ \chi(R) &= -\frac{\partial R}{\partial D} = \frac{(\sigma_R^2 R^2 + \sigma_K^2)R}{\gamma^{-1}\sigma_R^2\sigma_C^2\nu R^3 + (\sigma_R^2K + 2\gamma^{-1}\sigma_K^2\sigma_C^2\nu)R + \sigma_K^2D_{\text{eff}}}. \end{aligned} \quad (\text{A.25})$$

Note that to know the statistics of N , we should know the statistics of R before, but information for N is requisites to know the statistics of R . It means that they depend on themselves and make self-consistent relations.

Now, we obtain the self-consistent equations for seven macroscopic quantities as follows:

$$\begin{aligned} \phi_S &= \int_{+0}^{\infty} dN P(N), \\ \langle N \rangle &= \int_{+0}^{\infty} dN N P(N), \\ \langle N^2 \rangle &= \int_{+0}^{\infty} dN N^2 P(N), \\ \nu &= \langle \nu(N) \rangle = \int_{+0}^{\infty} dN \nu(N) P(N), \\ \langle R \rangle &= \int_{+0}^{\infty} dR R P(R), \\ \langle R^2 \rangle &= \int_{+0}^{\infty} dR R^2 P(R), \\ \chi &= \langle \chi(R) \rangle = \int_{+0}^{\infty} dR \chi(R) P(R). \end{aligned} \quad (\text{A.26})$$

For nonzero σ_h , the Jacobian term of $P(N)$ in Eq. (A.24) becomes zero when $N = -\sigma_g^2 h_{\text{eff}}/\sigma_h^2 g_{\text{eff}}$. This result implies that the consumer species are forbidden to have abundance value $N = -\sigma_g^2 h_{\text{eff}}/\sigma_h^2 g_{\text{eff}}$ because the value gives zero probability. The meaning of this forbidden value of N remains a question. For zero σ_h , however, the forbidden value of N disappears, because $P(N)$ in Eq. (A.24) becomes a simple truncated Gaussian distribution as

$$P(N) = \frac{h_{\text{eff}}}{\sqrt{2\pi}\sigma_g} \exp \left[-\frac{(h_{\text{eff}}N - g_{\text{eff}})^2}{2\sigma_g^2} \right] \quad \text{for } N > 0. \quad (\text{A.27})$$

Figure B7-B12 show $P(N)$ and $P(R)$ with and without intraspecific suppression in three different environments for different σ_C . In this case, the response function ν becomes much simpler as $\nu = \int_{+0}^{\infty} dN \nu(N)P(N) = \phi_S/h_{\text{eff}}$.

From our results, we obtain a relation between the relative diversity S^*/M^* and other parameters as

$$S^*/M^* = \gamma^{-1}\phi_S = \gamma^{-1}h_{\text{eff}}\nu = \gamma^{-1}(h + \sigma_C^2\chi)\nu. \quad (\text{A.28})$$

The S^*/M^* also can be evaluated by integrating $P(N)$ from $+0$ to ∞ as

$$S^*/M^* = \gamma^{-1}\phi_S = \gamma^{-1} \int_{+0}^{\infty} dN P(N) = \frac{\gamma^{-1}}{2} \left[1 + \text{erf} \left(\frac{g_{\text{eff}}}{\sqrt{2}\sigma_g} \right) \right], \quad (\text{A.29})$$

where $\text{erf}(x)$ indicates the error function. We notice that S^*/M^* is determined by the ratio between g_{eff} and σ_g , and numerically validate Eq. (A.29) for different K and h varying σ_C as displayed in Fig. A1.

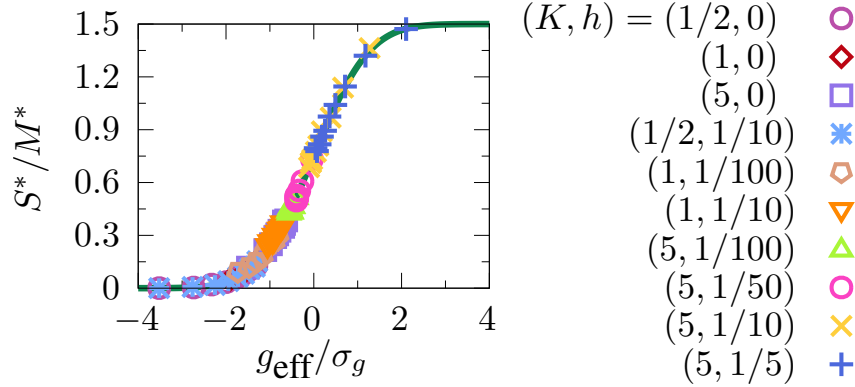


Fig A1. Relative diversity S^*/M^* for different (K, h) sets. For each (K, h) , σ_C varies in range $[0, 1]$ with constant increment $d\sigma_C = 0.1$. The green solid line behind the symbols indicates $\gamma^{-1}/2 [1 + \text{erf}(g_{\text{eff}}/\sqrt{2}\sigma_g)]$.

A.4. Bounds of the relative diversity

In Eq. (A.28), the term $\gamma^{-1}\sigma_C^2\chi\nu$ increases in σ_C starting from 0 at $\sigma_C = 0$, and thus S^*/M^* has its minimum value at $\sigma_C = 0$, and the maximum value as $\sigma_C \rightarrow \infty$. We approximately evaluate $\gamma^{-1}\sigma_C^2\chi\nu$ taking the limit of infinite σ_C to determine the maximum value as

$$\begin{aligned} \lim_{\sigma_C \rightarrow \infty} \gamma^{-1}\sigma_C^2\chi\nu &= \lim_{\sigma_C \rightarrow \infty} \int_{+0}^{\infty} dR \gamma^{-1}\sigma_C^2\nu\chi(R)P(R) \\ &= \lim_{\sigma_C \rightarrow \infty} \int_{+0}^{\infty} dR \frac{\gamma^{-1}\sigma_C^2\nu R}{\sqrt{2\pi(\sigma_R^2 R^2 + \sigma_K^2)}} \exp \left[-\frac{(\gamma^{-1}\sigma_C^2\nu R^2 + D_{\text{eff}}R - K)^2}{2(\sigma_R^2 R^2 + \sigma_K^2)} \right] \\ &= \lim_{\sigma_C \rightarrow \infty} \int_{+0}^{\infty} dR \frac{\gamma^{-1}\sigma_C^2\nu R}{\sqrt{2\pi[(\gamma^{-1}\sigma_C^2\langle N^2 \rangle + \sigma_D^2)R^2 + \sigma_K^2]}} \exp \left[-\frac{(\gamma^{-1}\sigma_C^2\nu R^2 + D_{\text{eff}}R - K)^2}{2[(\gamma^{-1}\sigma_C^2\langle N^2 \rangle + \sigma_D^2)R^2 + \sigma_K^2]} \right] \\ &\approx \lim_{\sigma_C \rightarrow \infty} \int_{+0}^{\infty} dR \frac{\gamma^{-1/2}\sigma_C\nu}{\sqrt{2\pi\langle N^2 \rangle}} \left(1 - \frac{\sigma_D^2 R^2 + \sigma_K^2}{2\gamma^{-1}\sigma_C^2\langle N^2 \rangle R^2} \right) \\ &\quad \times \exp \left[-\frac{\gamma^{-1}\sigma_C^2\nu^2 R^2}{2\langle N^2 \rangle} \left(1 + \frac{D_{\text{eff}}R - K}{\gamma^{-1}\sigma_C^2\nu R} \right)^2 \left(1 - \frac{\sigma_D^2 R^2 + \sigma_K^2}{\gamma^{-1}\sigma_C^2\langle N^2 \rangle R^2} \right) \right] \\ &\approx \lim_{\sigma_C \rightarrow \infty} \int_{+0}^{\infty} dR \frac{\gamma^{-1/2}\sigma_C\nu}{\sqrt{2\pi\langle N^2 \rangle}} \exp \left[-\frac{\gamma^{-1}\sigma_C^2\nu^2 R^2}{2\langle N^2 \rangle} \right] = \frac{1}{2}. \end{aligned} \quad (\text{A.30})$$

In the last approximation step, we used the fact that $\sigma_C^2 \nu$ and $\sigma_C^2 \langle N^2 \rangle$ diverge as $\sigma_C \rightarrow \infty$. Finally, we determine the bounds of S^*/M^* as follows:

$$\gamma^{-1} h \nu \leq S^*/M^* < \gamma^{-1} h \nu + 1/2. \quad (\text{A.31})$$

B. NUMERICAL SIMULATION RESULTS

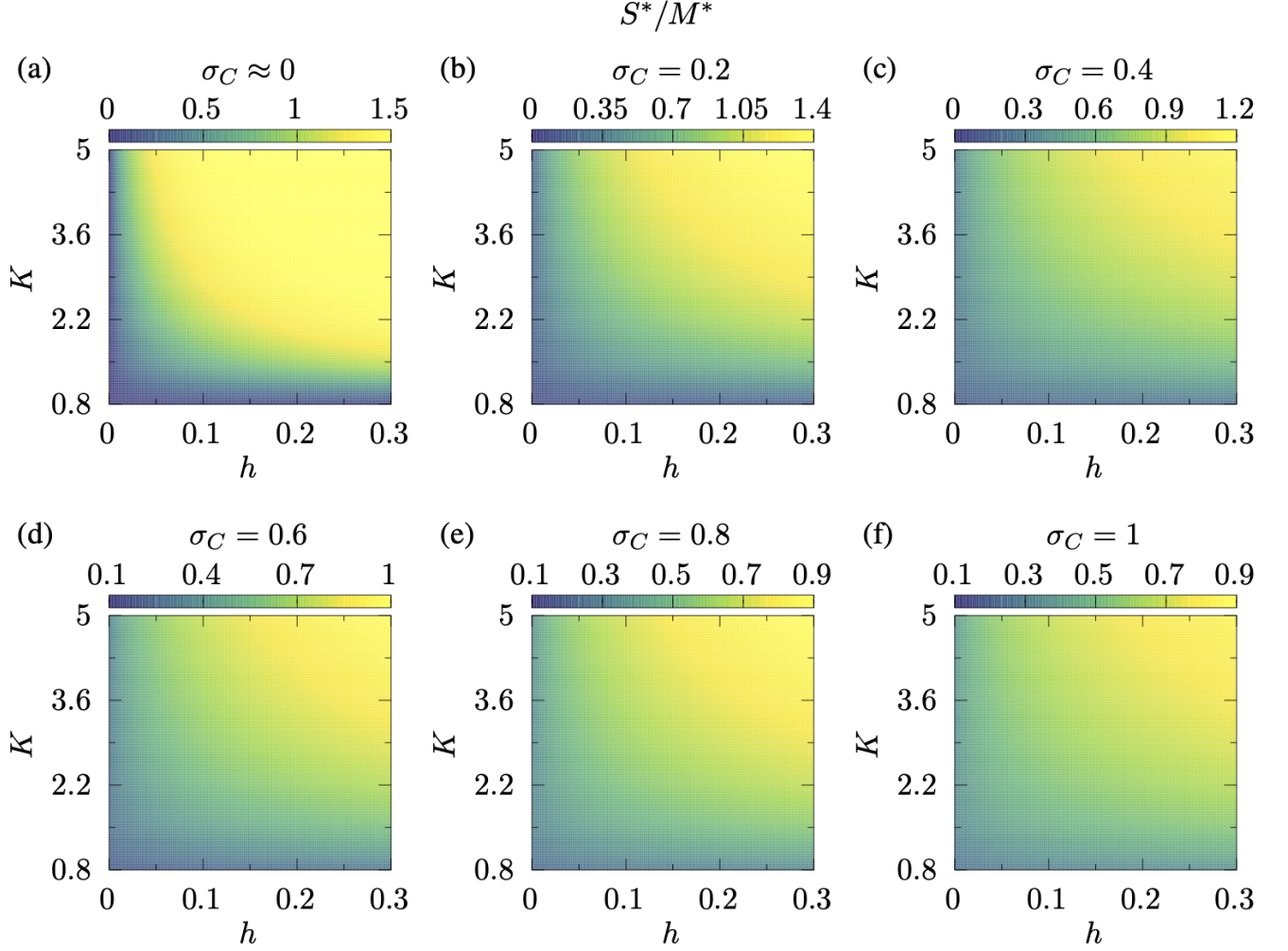


Fig B1. Relative diversity S^*/M^* in (h, K) -plane for six different consumption rate deviations of $\sigma_C = 0.004, 0.2, 0.4, 0.6, 0.8,$ and 1 .

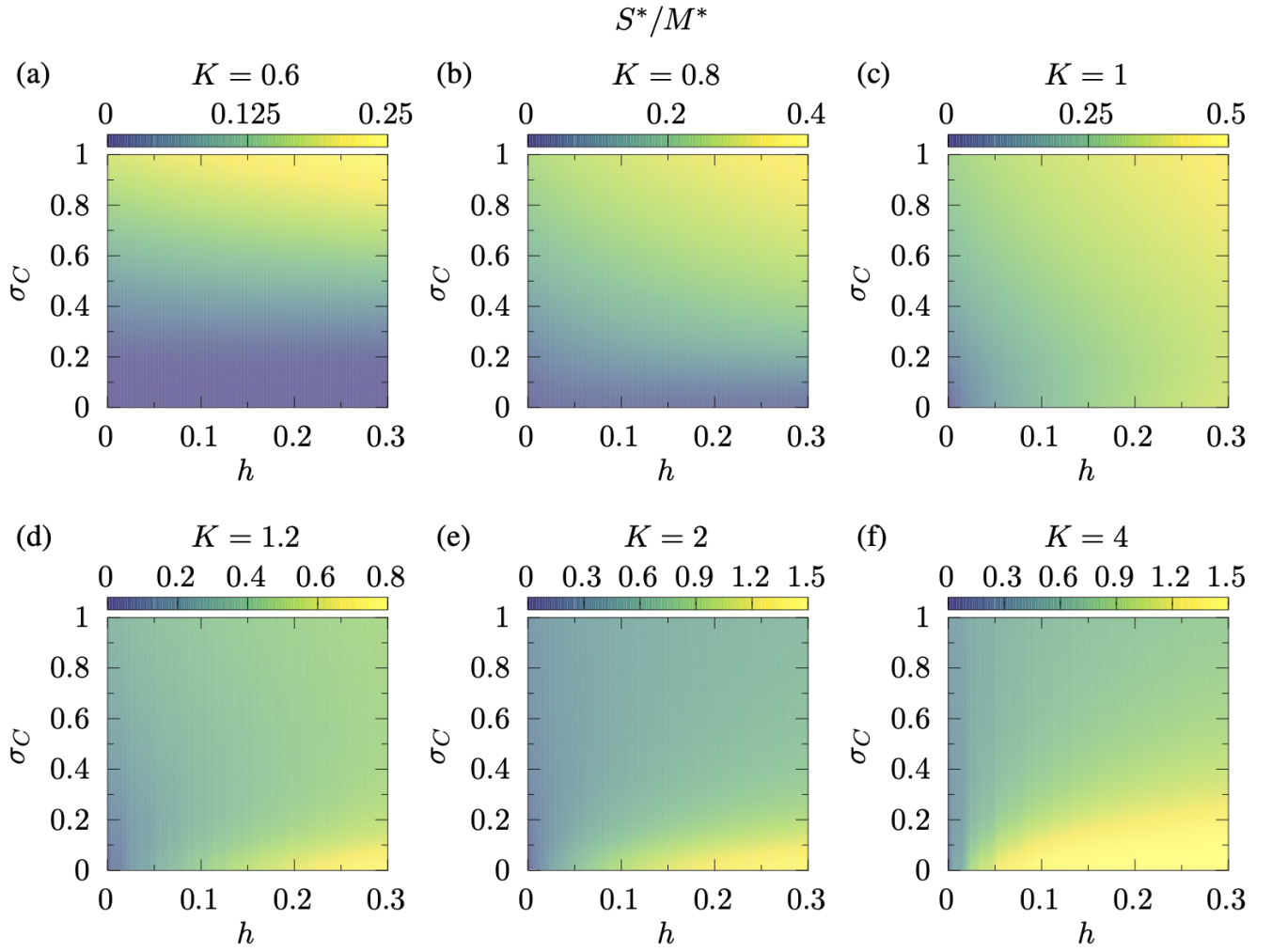


Fig B2. Relative diversity S^*/M^* in (h, σ_C) -plane in different environments of $K = 0.6, 0.8, 1, 1.2, 2,$ and 4 .

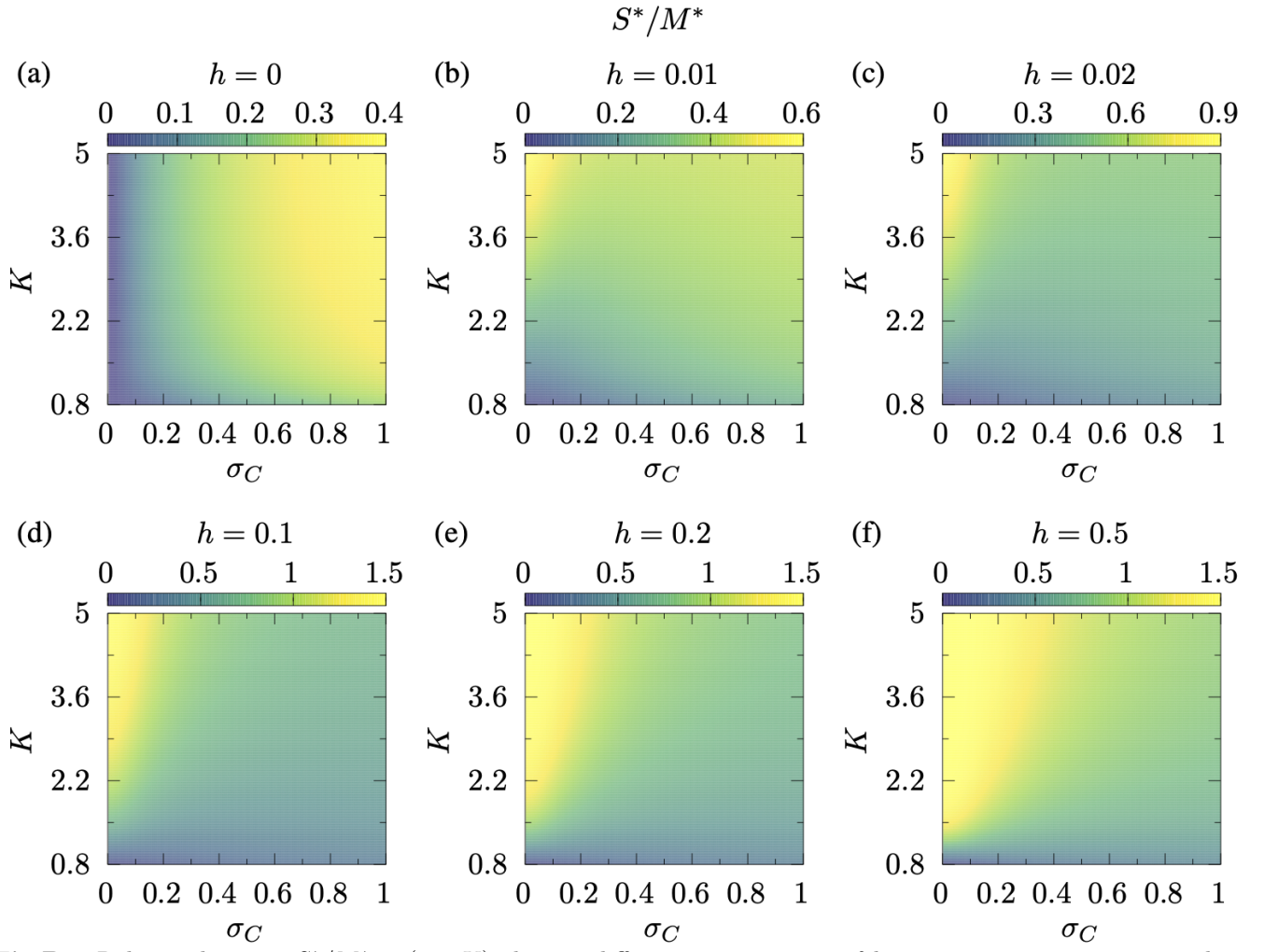


Fig B3. Relative diversity S^*/M^* in (σ_C, K) -plane in different environments of $h = 0, 0.01, 0.02, 0.1, 0.2,$ and 0.5 .

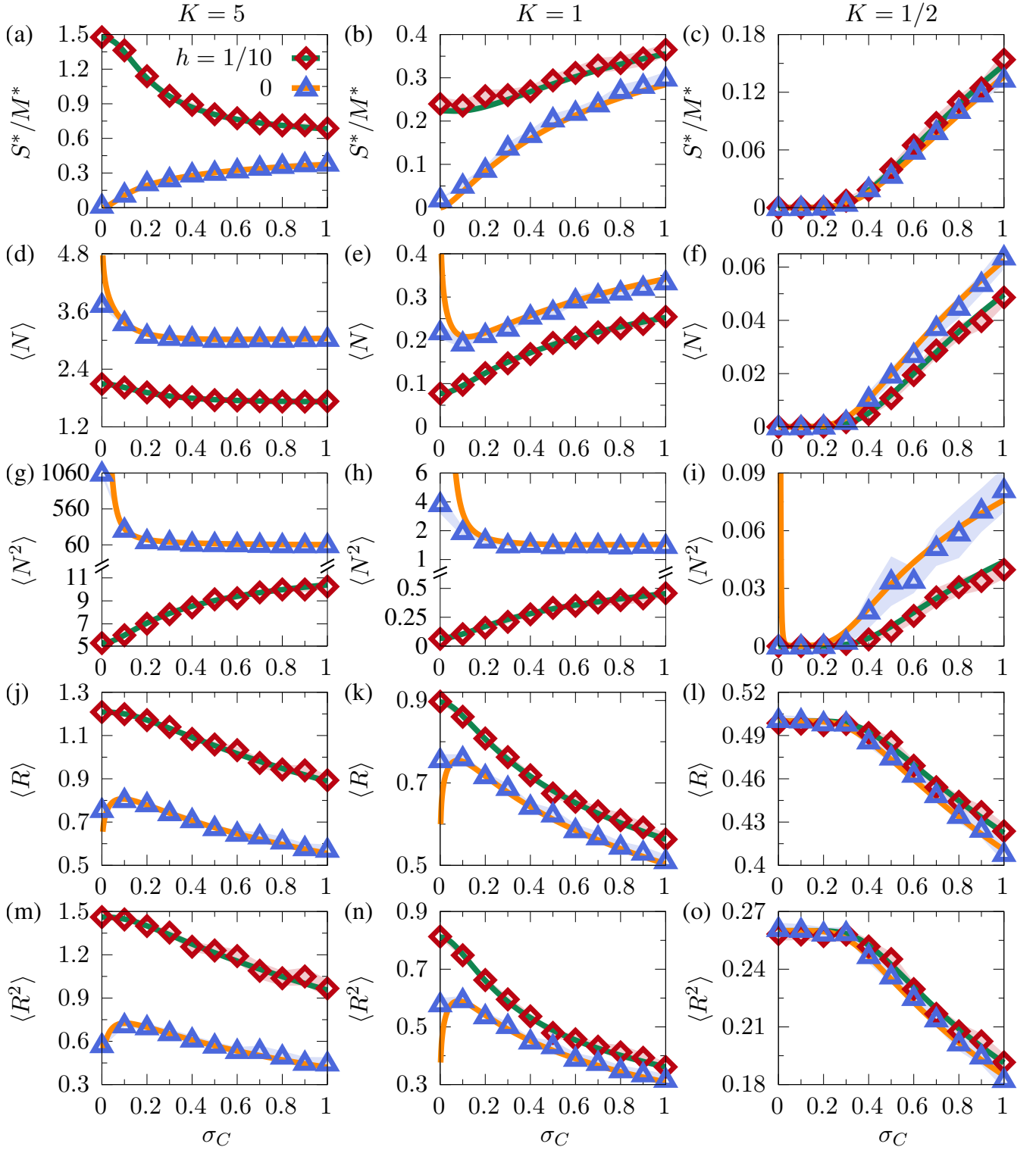


Fig B4. [(a), (b), and (c)] Relative diversity S^*/M^* of consumers, [(d), (e), and (f)] average consumer abundance $\langle N \rangle$, [(g), (h), and (i)] average consumer abundance square $\langle N^2 \rangle$, [(j), (k), and (l)] average resource abundance $\langle R \rangle$, and [(m), (n), and (o)] average resource abundance square $\langle R^2 \rangle$ versus consumption rate deviation σ_C in [(a), (d), (g), (j), and (m)] resource-rich ($K = 5$), [(b), (e), (h), (k), and (n)] resource-moderate ($K = 1$), and [(c), (f), (i), (l), and (o)] resource-poor ($K = 1/2$) environments. The solid lines are obtained from solving self-consistent equations, and the symbols are obtained from numerical simulations averaging over 50 different realizations. The colored shades indicate twice the standard error.

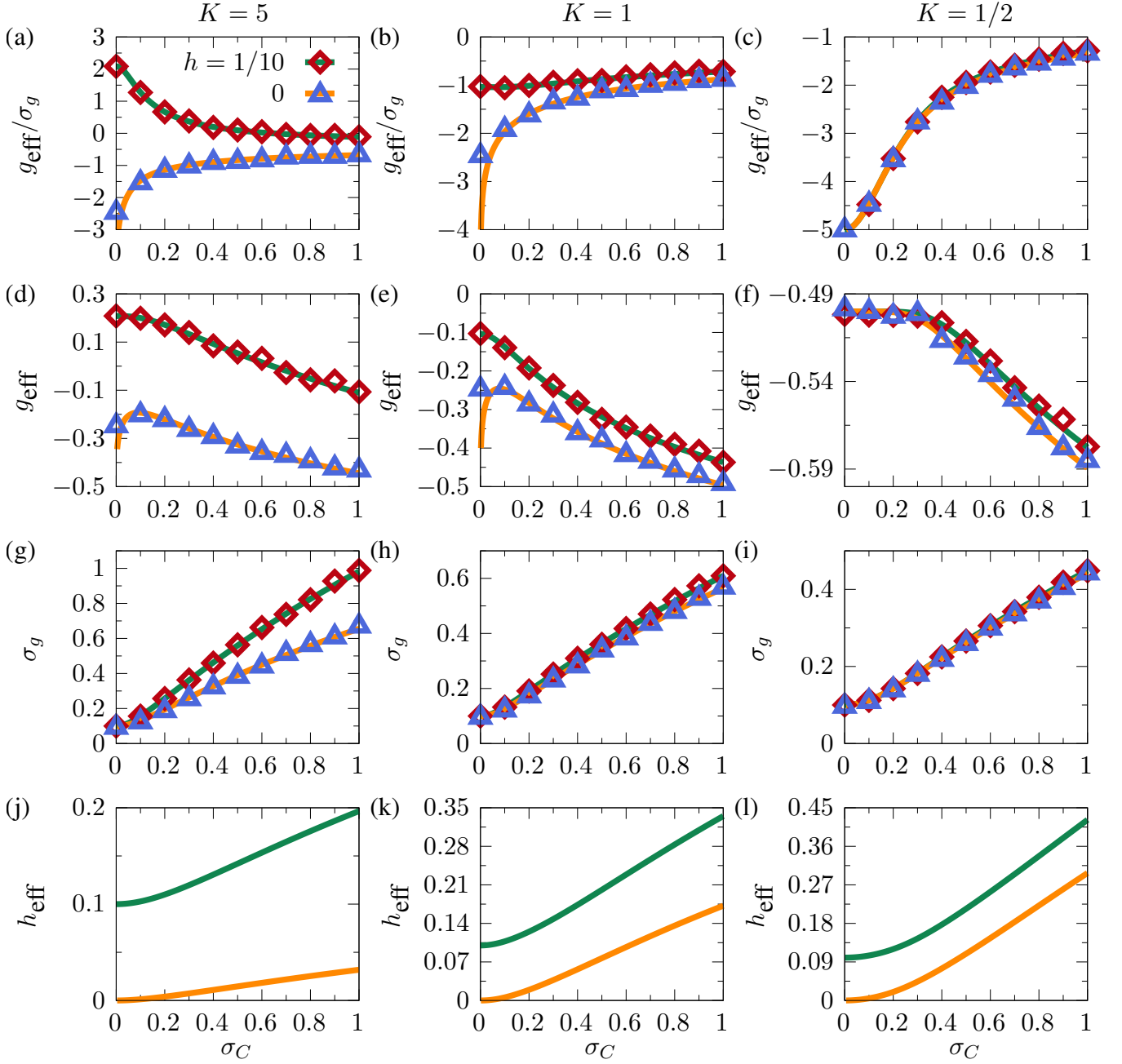


Fig B5. [(a), (b), and (c)] Ratio between effective growth rate g_{eff} and deviation σ_g in growth rate, [(d), (e) and (f)] g_{eff} , [(g), (h) and (i)] σ_g , and [(j), (k), and (l)] effective intraspecific suppression coefficient h_{eff} versus consumption rate deviation σ_C for without ($h = 0$), and with ($h = 1/10$) intraspecific suppression in [(a), (d), (g), and (j)] resource-rich ($K = 5$), [(b), (e), (h), and (k)] resource-moderate ($K = 1$), and [(c), (f), (i), and (l)] resource-poor ($K = 1/2$) environments. The green and yellow solid lines indicate the analytic results with and without intraspecific suppression, respectively. The symbols are obtained from numerical simulations averaging over 50 independent realizations.

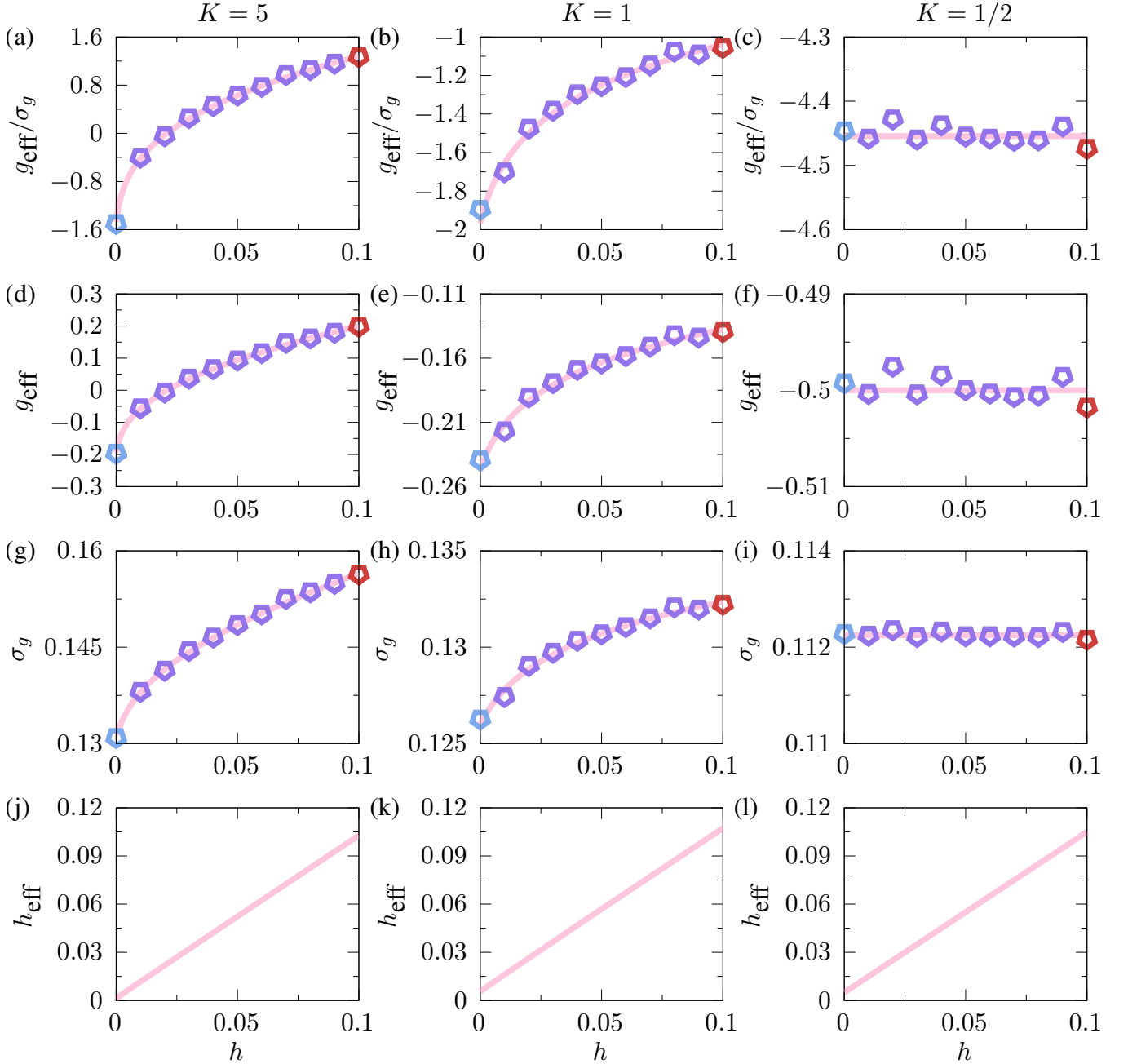


Fig B6. [(a), (b), and (c)] Ratio between effective growth rate g_{eff} and deviation σ_g in growth rate, [(d), (e) and (f)] g_{eff} , [(g), (h) and (i)] σ_g , and [(j), (k), and (l)] effective intraspecific suppression coefficient h_{eff} versus intraspecific suppression coefficient h for $\sigma_C = 1/10$ in [(a), (d), (g), and (j)] resource-rich ($K = 5$), [(b), (e), (h), and (k)] resource-moderate ($K = 1$), and [(c), (f), (i), and (l)] resource-poor ($K = 1/2$) environments. The pink solid line denotes the analytic result. The symbols are obtained from averaging over 50 independent realizations. In the resource-poor environment, the number of surviving consumer species is too small, thus, the symbols quite deviate from analytic results.

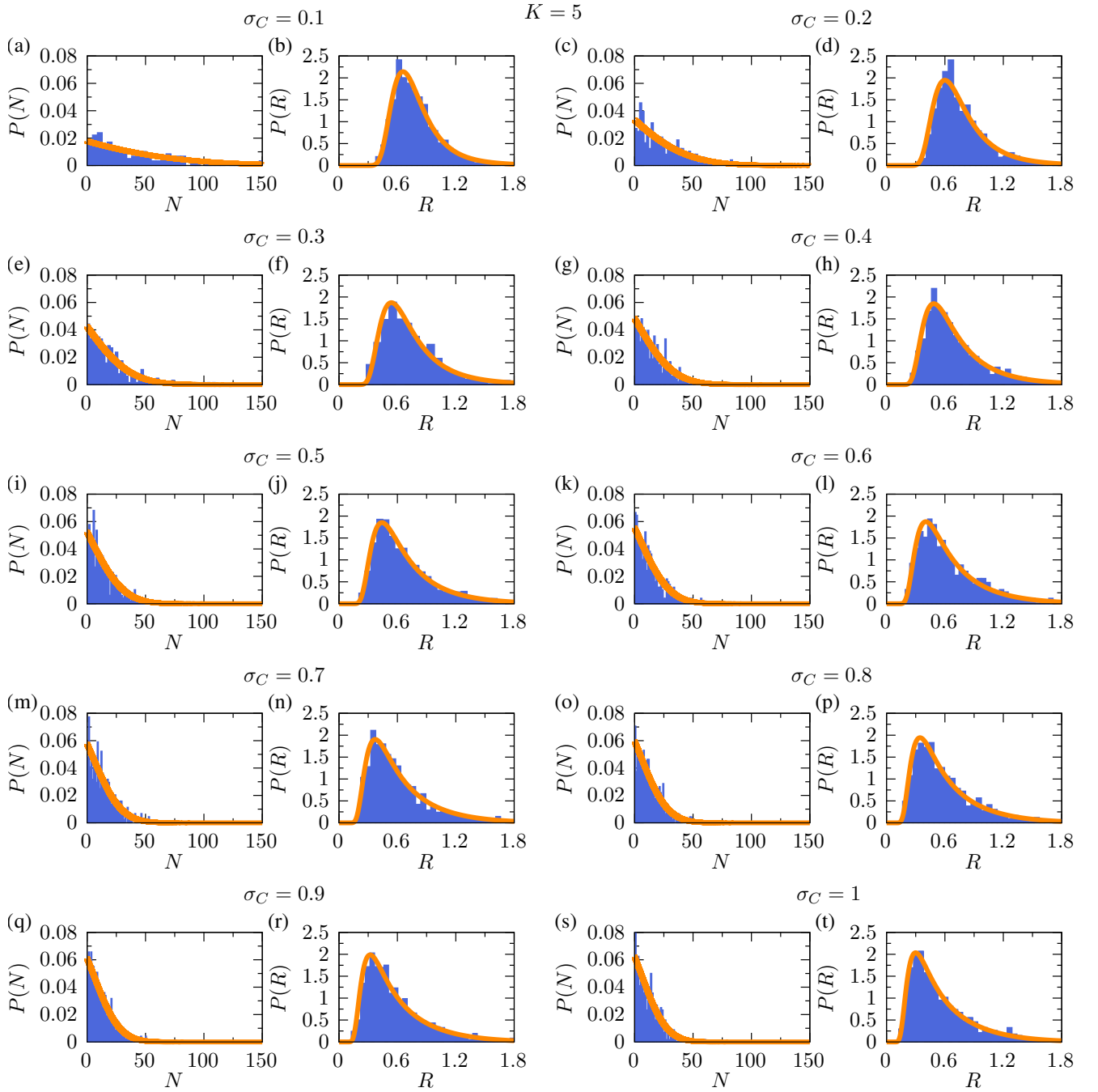


Fig B7. Consumer and resource abundance distributions without intraspecific suppression ($h = 0$) in the resource-rich ($K = 5$) environment for different σ_C .

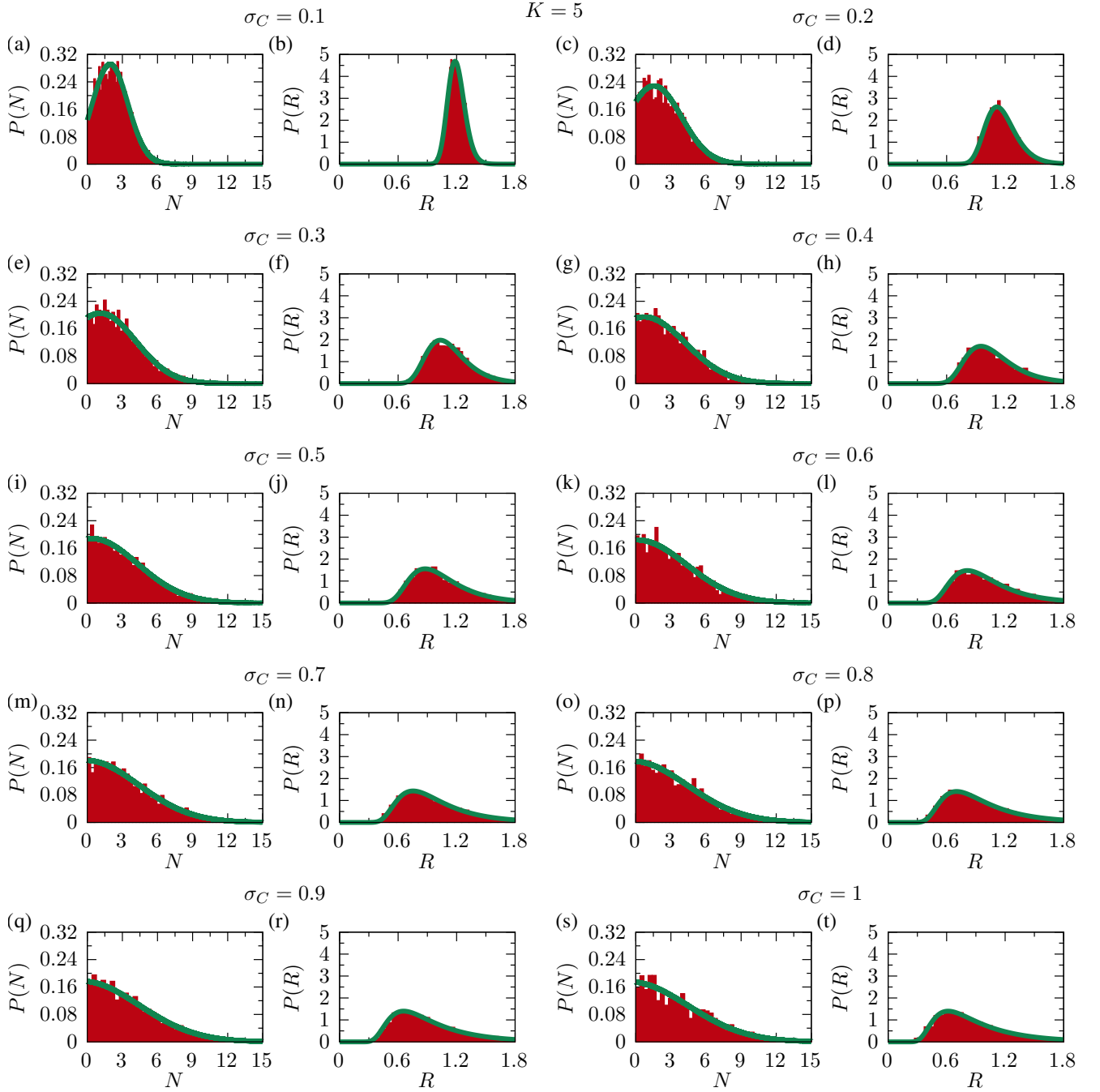


Fig B8. Consumer and resource abundance distributions with intraspecific suppression ($h = 1/10$) in the resource-rich ($K = 5$) environment for different σ_C .

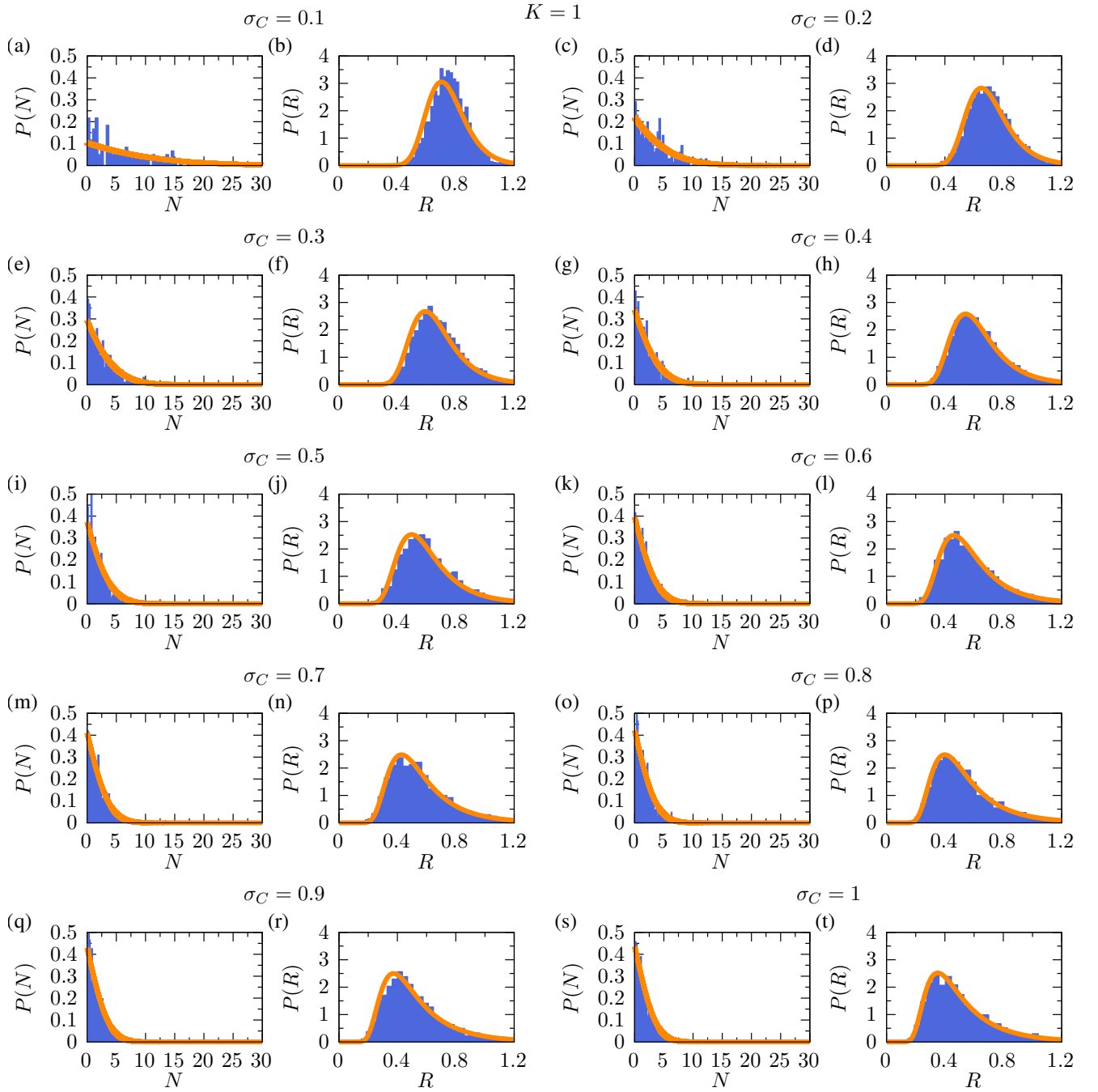


Fig B9. Consumer and resource abundance distributions without intraspecific suppression ($h = 0$) in the resource-moderate ($K = 1$) environment for different σ_C .

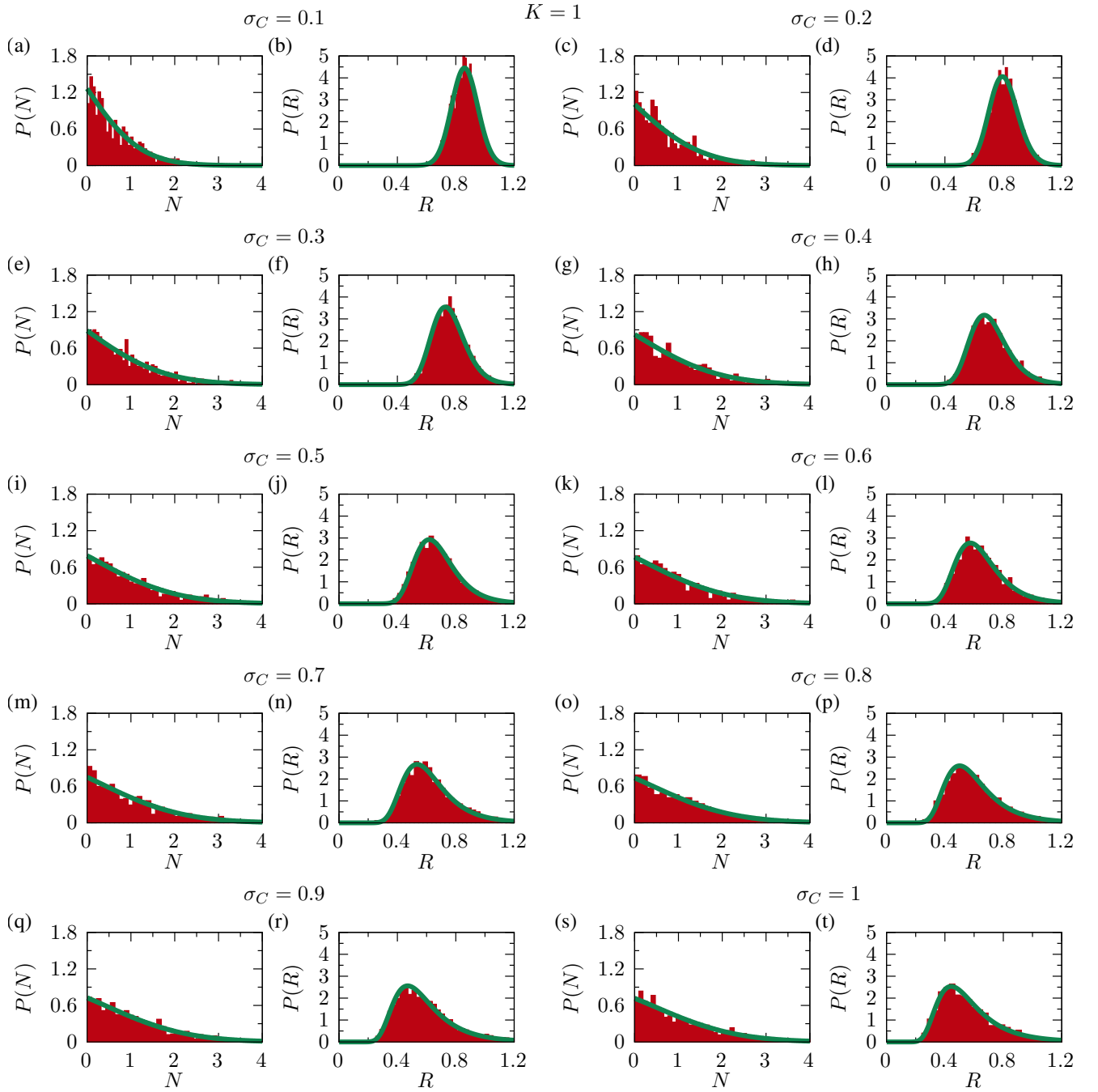


Fig B10. Consumer and resource abundance distributions with intraspecific suppression ($h = 1/10$) in the resource-moderate ($K = 1$) environment for different σ_C .

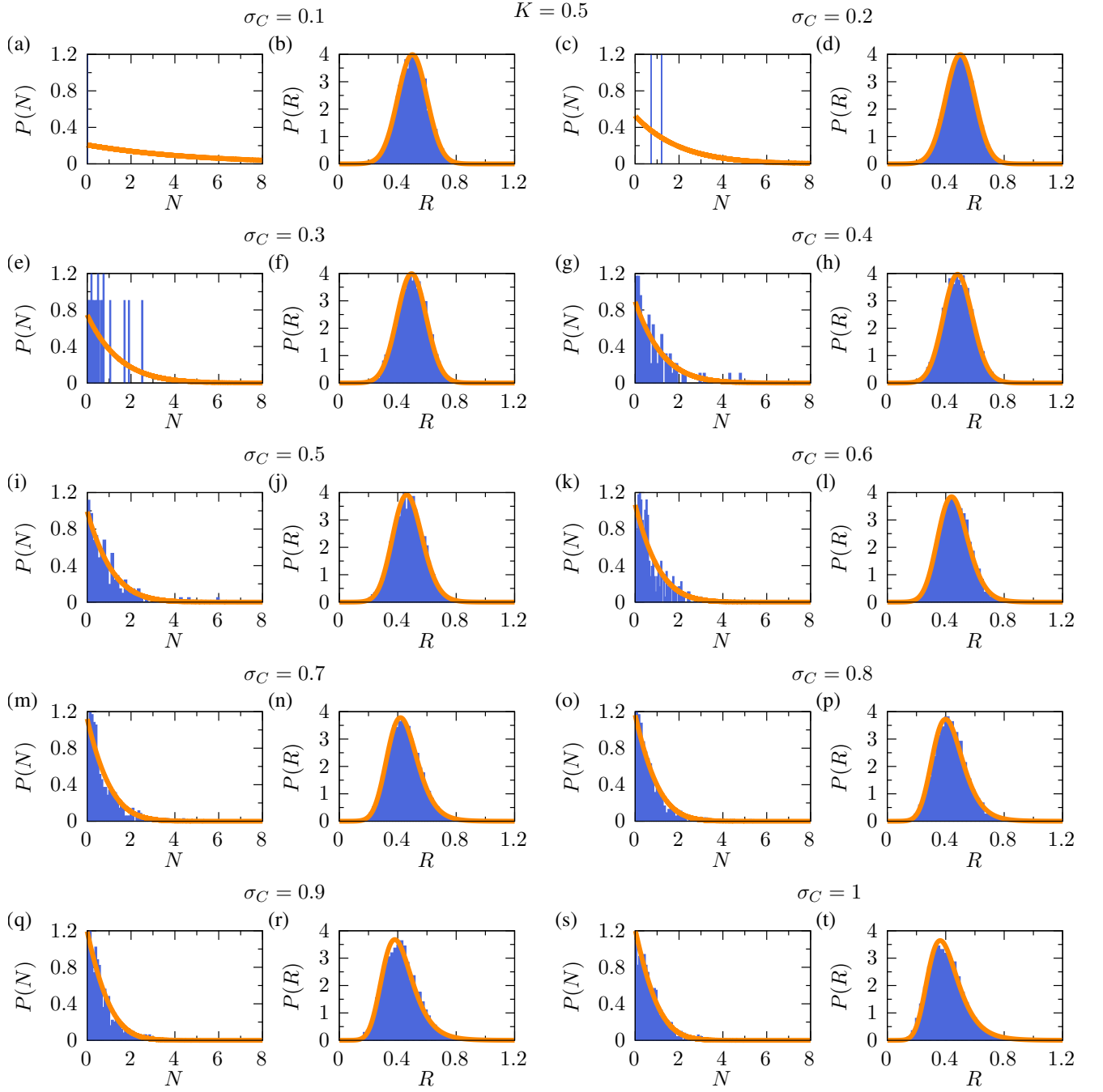


Fig B11. Consumer and resource abundance distributions without intraspecific suppression ($h = 0$) in the resource-poor ($K = 1/2$) environment for different σ_C . For $\sigma_C \leq 0.3$, the surviving probability of consumers is too low to get enough data points to fit well the truncated Gaussian distribution for N .

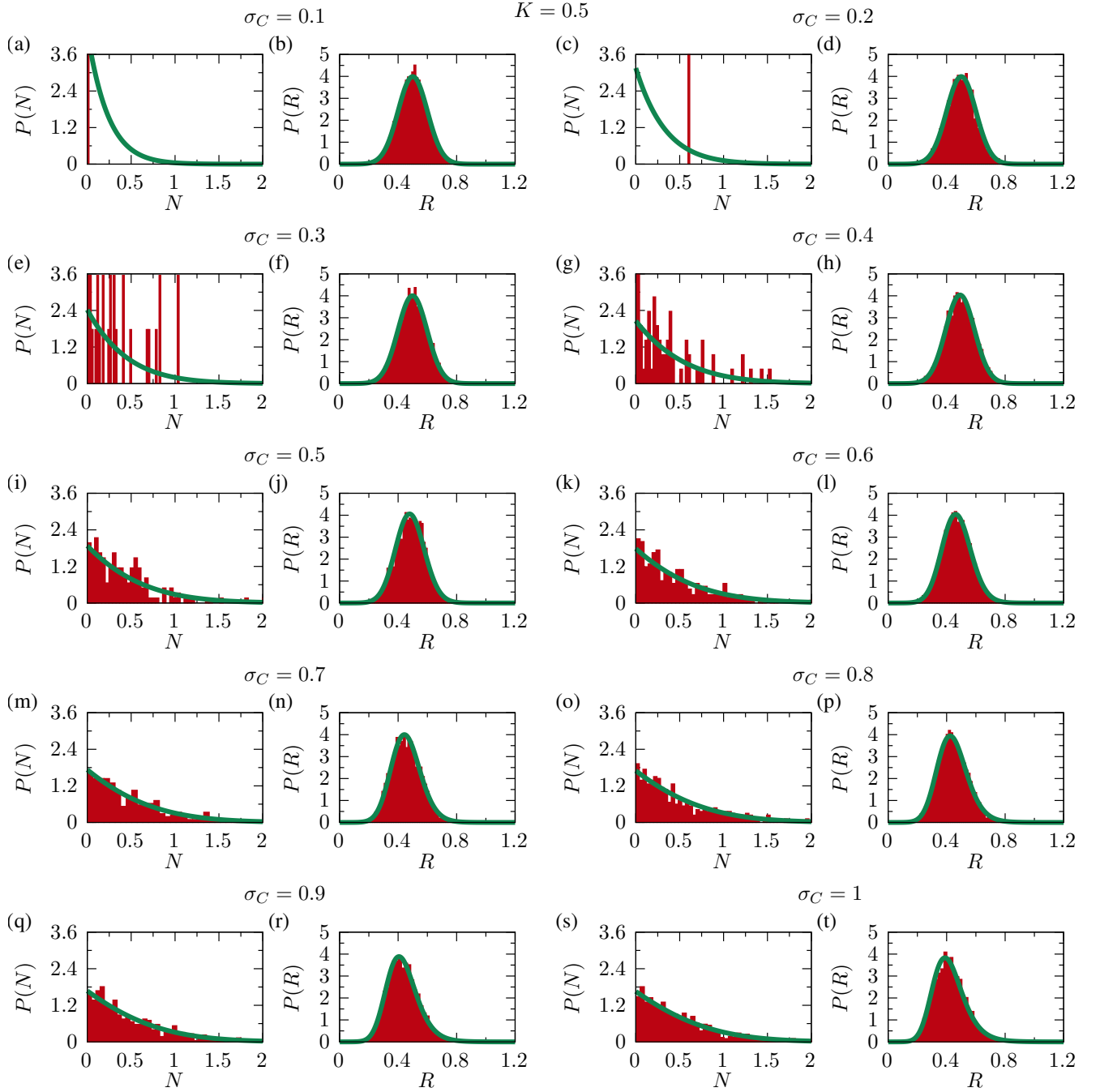


Fig B12. Consumer and resource abundance distributions with intraspecific suppression ($h = 1/10$) in the resource-poor ($K = 1/2$) environment for different σ_C . For $\sigma_C \leq 0.4$, the number of data points is not sufficient to fit well the truncated Gaussian distribution for N .

C. SELF-RENEWING RESOURCES

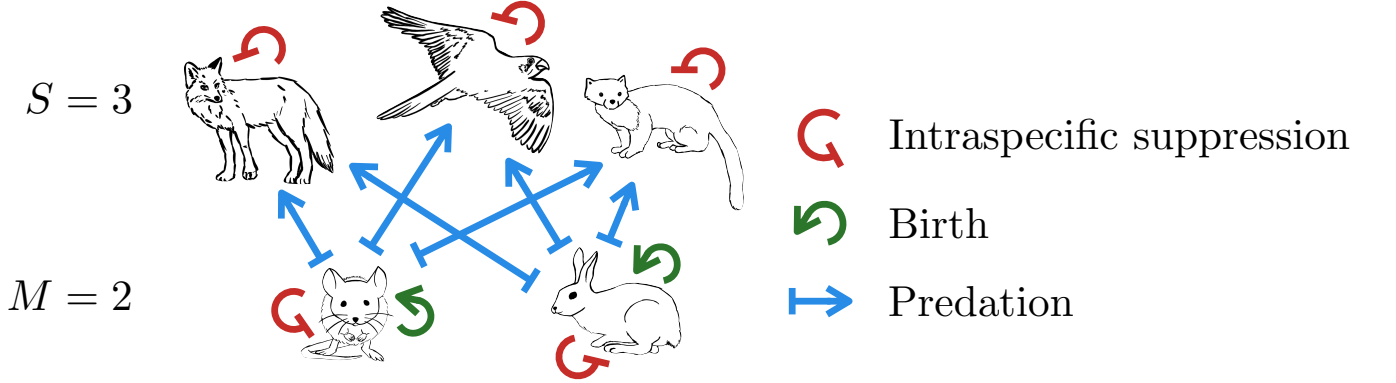


Fig C1. Schematic figure of an ecological system that consists of three predators ($S = 3$) and two self-renewing prey species ($M = 2$). Different from the externally supplied resources, prey species give birth and grow by themselves.

The GCRM for self-renewing resources without intraspecific suppression has been well studied [1]. In this section, the model with intraspecific suppression is dealt with. The GCRM for self-renewing resources with intraspecific suppression is written as follows:

$$\begin{aligned} \dot{N}_i &= N_i \left(\sum_{\alpha} C_{i\alpha} R_{\alpha} - m_i - h_i N_i \right), & i = 1, 2, \dots, S, \\ \dot{R}_{\alpha} &= R_{\alpha} \left(r_{\alpha} - d_{\alpha} R_{\alpha} - \sum_i N_i C_{i\alpha} \right), & \alpha = 1, 2, \dots, M, \end{aligned} \quad (\text{C.1})$$

where r_{α} and d_{α} denote the reproduction rate and the intraspecific suppression coefficient of resource α , respectively.

Following the procedures in Sec. I, we get the result of

$$z_R = (r_{\text{eff}} - d_{\text{eff}}R) / \sqrt{\sigma_R^2 + \sigma_d^2 R^2} \quad \text{for } R > 0, \quad (\text{C.2})$$

where $r_{\text{eff}} (\equiv r - \gamma^{-1} \mu_C \langle N \rangle)$ is the effective growth rate of self-renewing resources, $d_{\text{eff}} (\equiv d + \gamma^{-1} \sigma_C^2 \nu)$ is the effective death rate of the resources, and $\sigma_R^2 (\equiv \sigma_r^2 + \gamma^{-1} \sigma_C^2 \langle N^2 \rangle)$ is the variance in the effective growth rate of the resources. The results for the consumer species are the same as described in Sec. I.

Using the change of variables in the probability distribution, we obtain the abundance distribution for self-renewing resources as

$$P(R) = \frac{1}{\sqrt{2\pi}} \left| \frac{\sigma_d^2 r_{\text{eff}} R + \sigma_R^2 d_{\text{eff}}}{(\sigma_d^2 R^2 + \sigma_R^2)^{3/2}} \right| \exp \left[-\frac{(d_{\text{eff}}R - r_{\text{eff}})^2}{2(\sigma_d^2 R^2 + \sigma_R^2)} \right] \quad \text{for } R > 0, \quad (\text{C.3})$$

and the response function as $\chi(R) = \partial R / \partial r = (\sigma_R^2 + \sigma_d^2 R^2) / (\sigma_R^2 d_{\text{eff}} + \sigma_d^2 r_{\text{eff}} R)$.

Note that for this type of resource, the resources can go extinct, which is different from the externally supplied resources. Thus, the surviving probability ϕ_M of resources should be considered, and it is calculated by $\phi_M = \int_{+0}^{\infty} dR P(R)$.

When we ignore the disorder in intraspecific suppression for resources ($\sigma_d = 0$), we obtain the truncated Gaussian resource abundance distribution like consumer abundance as

$$P(R) = \frac{d_{\text{eff}}}{\sqrt{2\pi} \sigma_R} \exp \left[-\frac{(d_{\text{eff}}R - r_{\text{eff}})^2}{2\sigma_R^2} \right] \quad \text{for } R > 0. \quad (\text{C.4})$$

In this situation, the resource response function also becomes simpler as $\chi(R) = 1/d_{\text{eff}}$, and this result gives $\chi = \int_{+0}^{\infty} dR \chi(R) P(R) = \phi_M / d_{\text{eff}}$. Utilizing the relation between ϕ_M and χ , and ϕ_S and ν , we obtain

$$\phi_M - \gamma^{-1} \phi_S = d\chi - \gamma^{-1} h\nu, \quad (\text{C.5})$$

where d is the mean value of d_α . As $\phi_M - \gamma^{-1}\phi_S = (M^* - S^*)/M$, when coexisting consumers S^* is larger than the number of available prey M^* , $\phi_M - \gamma^{-1}\phi_S$ is negative. Thus by plotting $\phi_M - \gamma^{-1}\phi_S$ in Fig. C2, we investigate whether the intraspecific suppression enhances the relative diversity for self-renewing resources beyond the CEP bound 1. For highly reproductive prey ($r = 5$), the number of coexisting consumers is larger than the number of available prey in the system for $\sigma_C < 0.45$ with intraspecific suppression ($h = 1/10$) [Fig. C2(a)]. The effective parameters of consumer species g_{eff} , σ_g , and h_{eff} are displayed in Fig. C3. We fix the parameters $\gamma = 2/3$, $\mu_C = 1$, $m = 1$, $d = 1$, $\sigma_m = 1/10$, $\sigma_d = 0$, $\sigma_r = 1/10$, and $\sigma_h = 0$ throughout this section. For numerical simulations, we fix $S = 75$ and $M = 50$.

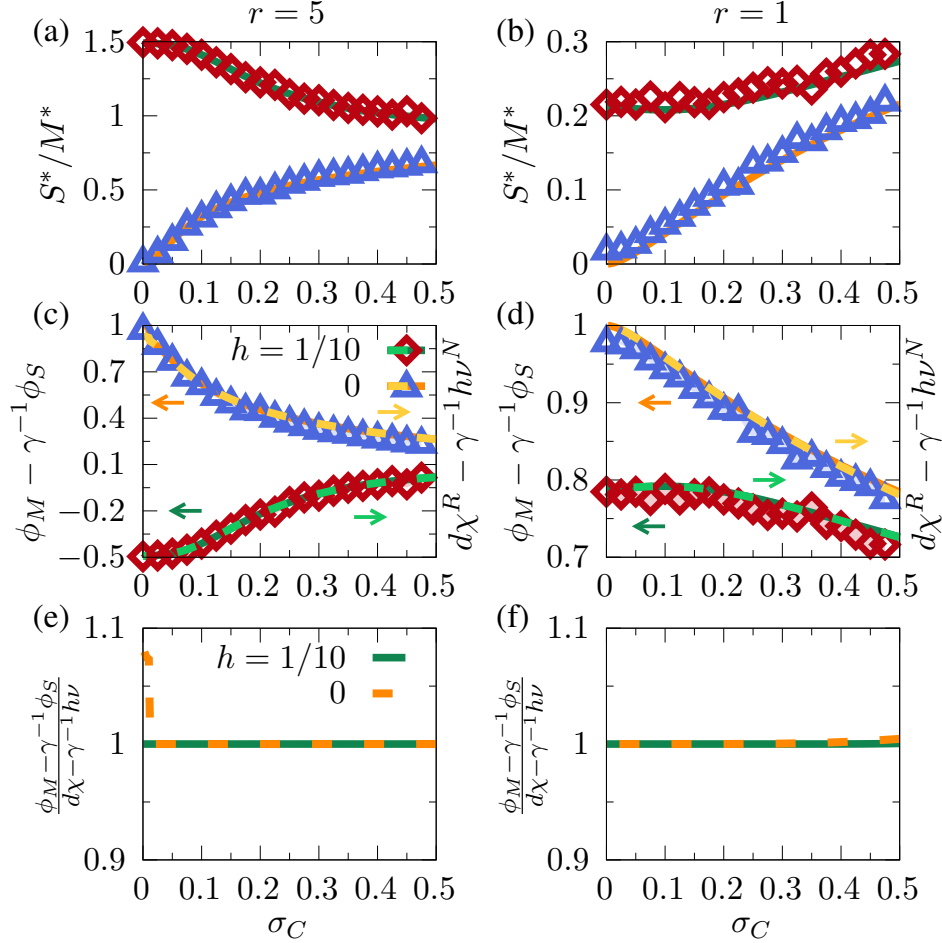


Fig C2. [(a) and (b)] The relative diversity S^*/M^* for (a) highly ($r = 5$) and (b) moderately ($r = 1$) reproductive prey without ($h = 0$) and with ($h = 1/10$) intraspecific suppression for consumers. [(c), (d), (e), and (f)] The relation we obtain for self-renewing resources for [(c) and (e)] highly and [(d) and (f)] moderately reproductive prey without and with intraspecific suppression for consumers. [(e) and (f)] We validate our results by dividing the left-hand side with the right-hand side of Eq. (C.5). The symbols are obtained by averaging over 50 independent realizations. In (c) and (d), the orange (yellow) and green (chartreuse) solid (dotted) lines denote the left-hand (right-hand) side without and with intraspecific suppression, respectively. Red and blue symbols are obtained by averaging over 50 independent realizations. In (e) and (f), the green solid line and orange dotted line indicate the ratio between left- and right-hand sides with and without intraspecific suppression, respectively.

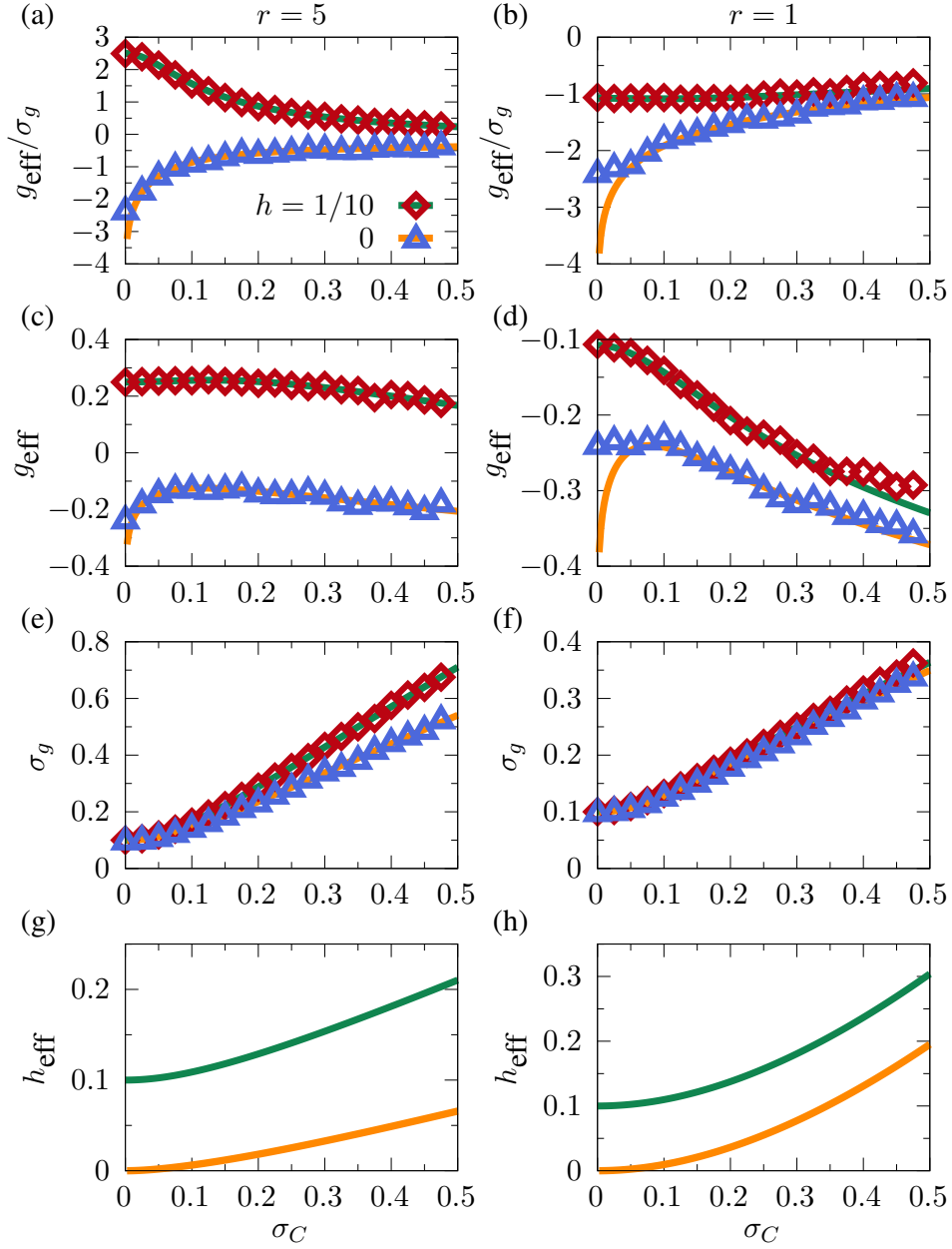


Fig C3. [(a) and (b)] The ratio between the effective growth rate g_{eff} of consumers and the deviation σ_g in the growth rate, [(c) and (d)] g_{eff} , [(e) and (f)] σ_g , and [(g) and (h)] the effective intraspecific suppression coefficient h_{eff} with ($h = 1/10$) and without ($h = 0$) intraspecific suppression for [(a), (c), (e), and (g)] highly ($r = 5$) and [(b), (d), (f), and (h)] moderately ($r = 1/2$) reproductive prey.

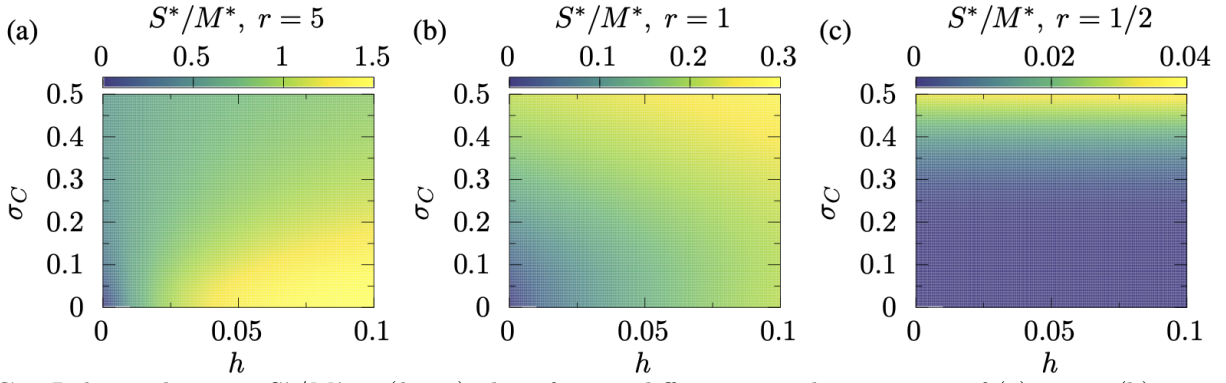


Fig C4. Relative diversity S^*/M^* in (h, σ_C) -plane for two different reproduction rates of (a) $r = 5$, (b) $r = 1$, and (c) $r = 1/2$. The relative diversity shows qualitatively the same behavior as that in the externally supplied resource.

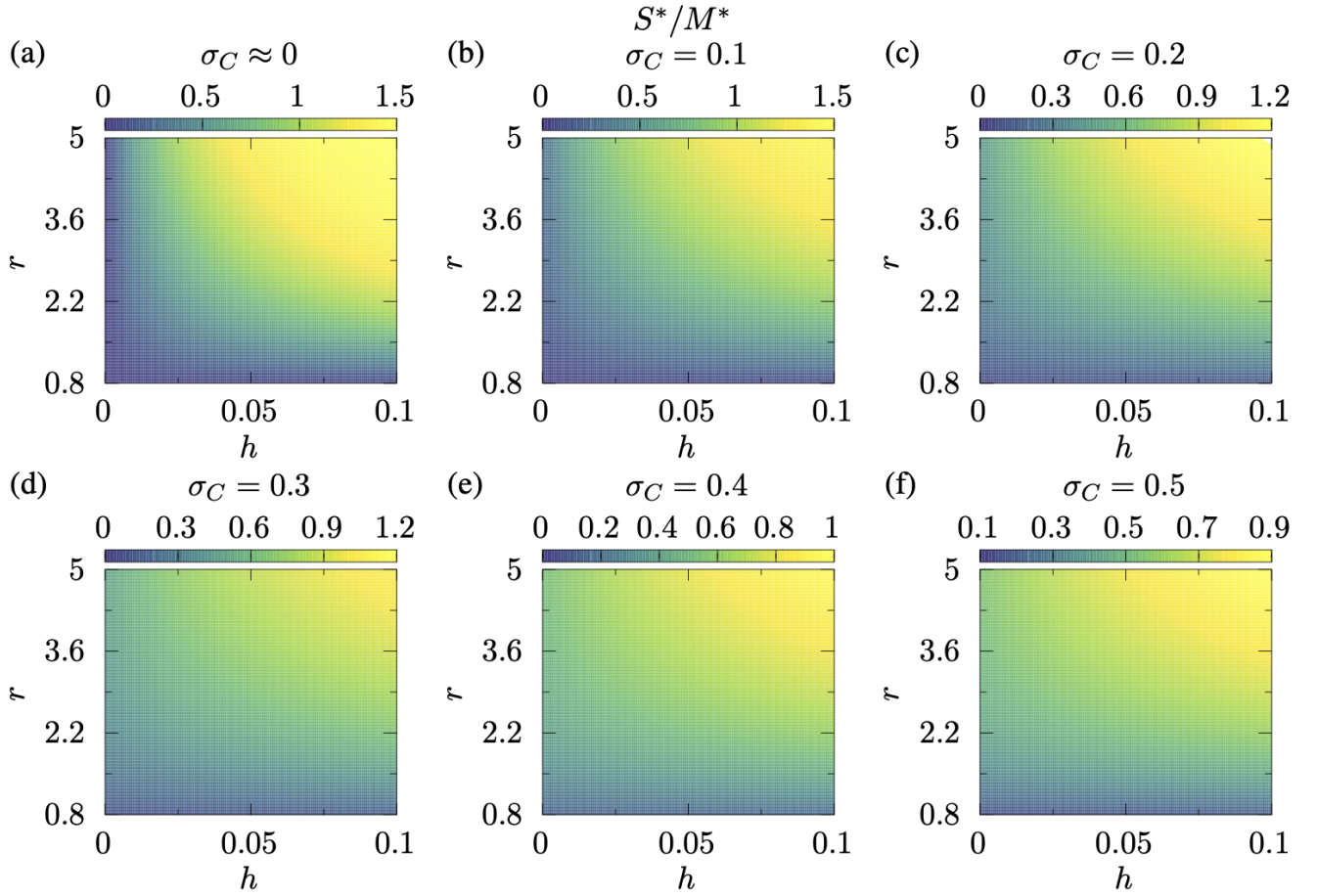


Fig C5. Relative diversity S^*/M^* in (h, r) -plane for six different consumption rate deviations of $\sigma_C = 0.004, 0.1, 0.2, 0.3, 0.4,$ and 0.5 .

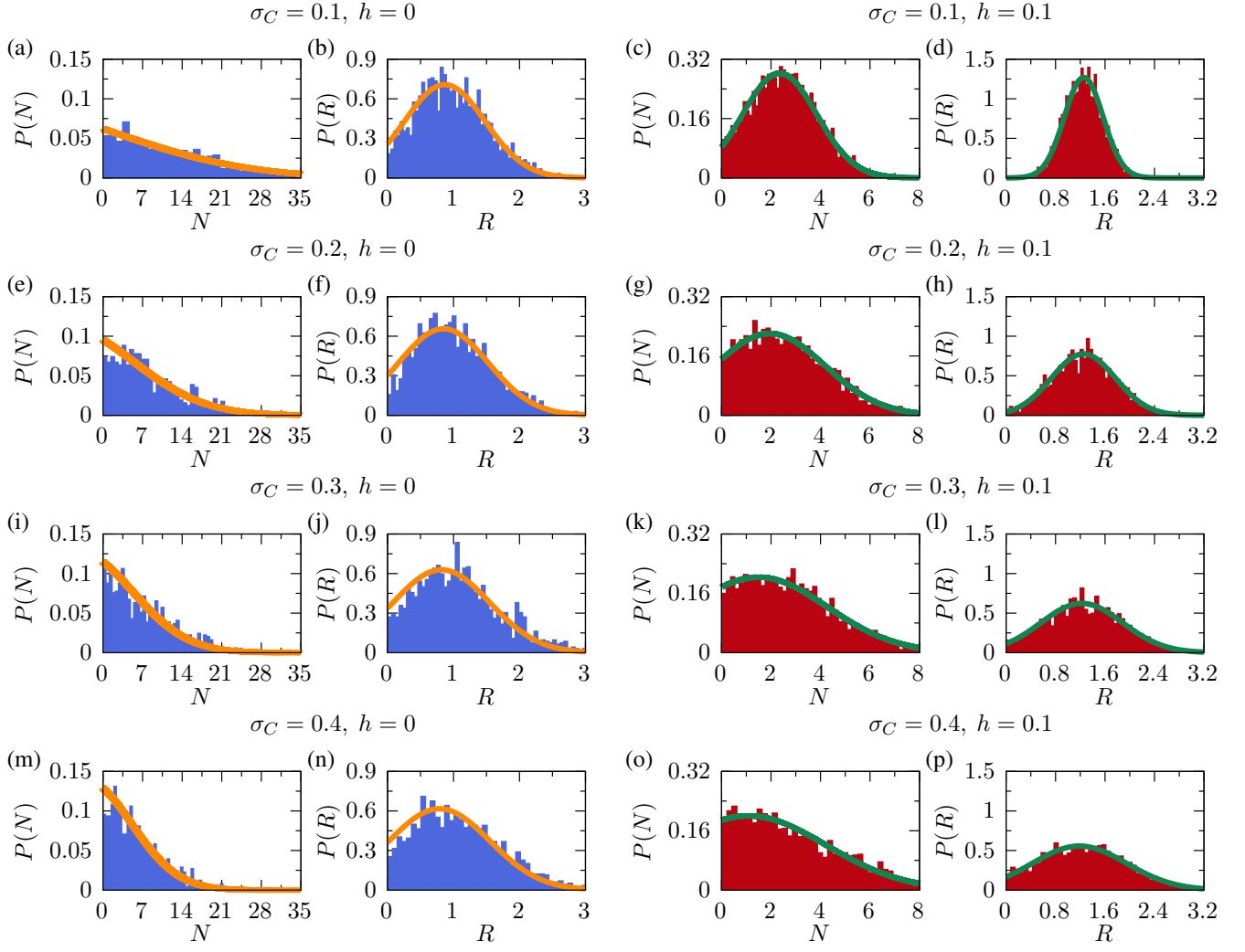
$r = 5$ 

Fig C6. Distributions without ($h = 0$) and with ($h = 1/10$) intraspecific suppression of consumers for highly ($r = 5$) reproductive prey.

$r = 1$

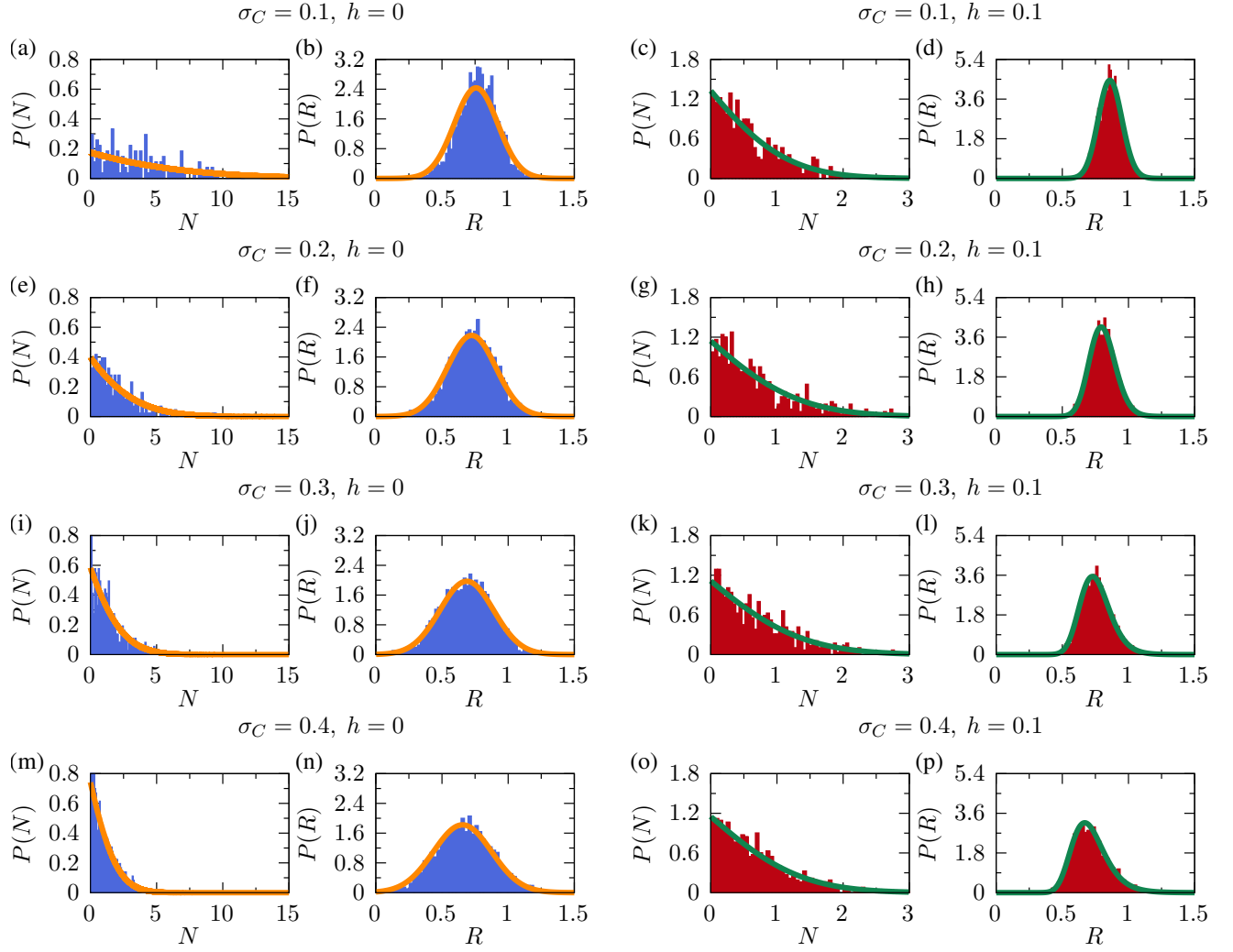


Fig C7. Distributions without ($h = 0$) and with ($h = 1/10$) intraspecific suppression of consumers for moderately ($r = 1$) reproductive prey.

D. THREE-TROPHIC LEVEL SYSTEMS

In this Section, we extend the model to describe three-trophic level systems, which consist of consumers, producers, and externally supplied abiotic resources, and obtain the abundance distributions for two consumers and externally supplied abiotic resource utilizing the method described in Sec. A. The ecological systems of three-trophic level can be described by

$$\begin{aligned}
 \dot{N}_i &= N_i \left(\sum_{\alpha} C_{i\alpha} R_{\alpha} - m_i - h_i N_i \right), & i = 1, 2, \dots, S, \\
 \dot{R}_{\alpha} &= R_{\alpha} \left(r_{\alpha} + \sum_{\gamma} G_{\alpha\gamma} A_{\gamma} - d_{\alpha} R_{\alpha} - \sum_i N_i C_{i\alpha} \right), & \alpha = 1, 2, \dots, M, \\
 \dot{A}_{\gamma} &= K_{\gamma} - \left(E_{\gamma} + \sum_{\alpha} R_{\alpha} G_{\alpha\gamma} \right) A_{\gamma}, & \gamma = 1, 2, \dots, L,
 \end{aligned} \tag{D.1}$$

where N_i , R_{α} , and A_{γ} indicate the abundance of consumer i , producer α , and resource γ , with fixed initial species ratios $\gamma = M/S$ and $\lambda = L/M$. Here, we introduce an additional consumption (grazing) matrix G , which indicates the relation between the producer α and the resource γ . E_{γ} indicates the degradation rate of the resource γ .

We obtain the relations that those three abundances should follow at the steady state likewise in Eq. (A.22),

$$\begin{aligned}
 0 &= N \left[g_{\text{eff}} - h_{\text{eff}} N + z_N \sqrt{\sigma_g^2 + \sigma_h^2 N^2} \right], \\
 0 &= R \left[r_{\text{eff}} - d_{\text{eff}} R + z_R \sqrt{\sigma_R^2 + \sigma_d^2 R^2} \right], \\
 0 &= K - E_{\text{eff}} - \lambda^{-1} \sigma_G^2 \chi A^2 + z_A \sqrt{\sigma_K^2 + \sigma_A^2 A^2},
 \end{aligned} \tag{D.2}$$

where the mean effective degradation rate is written as $E_{\text{eff}} \equiv E + \lambda^{-1} \mu_G \langle R \rangle$, and variance as $\sigma_A^2 \equiv \sigma_G^2 + \lambda^{-1} \sigma_G^2 \langle R^2 \rangle$. μ_G and σ_G indicate mean and deviation of G , respectively. h_{eff} , g_{eff} , and σ_g are defined in Sec. A A.3, but r_{eff} , d_{eff} , and σ_R^2 have an additional term from abiotic resource as $r_{\text{eff}} \equiv r - \gamma^{-1} \mu_C \langle N \rangle + \mu_G \langle A \rangle$, $d_{\text{eff}} \equiv d + \gamma^{-1} \sigma_C^2 \nu + \sigma_G^2 \theta$, and $\sigma_R^2 \equiv \sigma_r^2 + \gamma^{-1} \sigma_C^2 \langle N^2 \rangle + \sigma_G^2 \langle A^2 \rangle$, where $\theta = - \langle \frac{\partial A}{\partial E} \rangle = \left\langle \frac{(\sigma_A^2 A^2 + \sigma_K^2) A}{\lambda^{-1} \sigma_A^2 \sigma_G^2 \chi A^3 + (\sigma_A^2 K + 2\lambda^{-1} \sigma_K^2 \sigma_G^2 \chi) A + \sigma_K^2 E_{\text{eff}}} \right\rangle$ is the response function of externally supplied (abiotic) resource.

From Eq. (D.2), we obtain the abundance distributions for three-trophic level ecosystems in the same way described in Sec. A A.3 as follow,

$$\begin{aligned}
 P(N) &= \frac{1}{\sqrt{2\pi}} \left| \frac{\sigma_h^2 g_{\text{eff}} N + \sigma_g^2 h_{\text{eff}}}{(\sigma_h^2 N^2 + \sigma_g^2)^{3/2}} \right| \exp \left[- \frac{(h_{\text{eff}} N - g_{\text{eff}})^2}{2(\sigma_h^2 N^2 + \sigma_g^2)} \right], \quad \text{for } N > 0, \\
 P(R) &= \frac{1}{\sqrt{2\pi}} \left| \frac{\sigma_d^2 r_{\text{eff}} R + \sigma_R^2 d_{\text{eff}}}{(\sigma_d^2 R^2 + \sigma_R^2)^{3/2}} \right| \exp \left[- \frac{(d_{\text{eff}} R - r_{\text{eff}})^2}{2(\sigma_d^2 R^2 + \sigma_R^2)} \right], \quad \text{for } R > 0, \\
 P(A) &= \frac{1}{\sqrt{2\pi}} \left| \frac{\lambda^{-1} \sigma_A^2 \sigma_G^2 \chi A^3 + (\sigma_A^2 K + 2\lambda^{-1} \sigma_K^2 \sigma_G^2 \chi) A + \sigma_K^2 E_{\text{eff}}}{(\sigma_A^2 A^2 + \sigma_K^2)^{3/2}} \right| \\
 &\quad \times \exp \left[- \frac{(\lambda^{-1} \sigma_G^2 \chi A^2 + E_{\text{eff}} A - K)^2}{2(\sigma_A^2 A^2 + \sigma_K^2)} \right].
 \end{aligned} \tag{D.3}$$

-
- [1] M. Advani, G. Bunin, and P. Mehta, Statistical physics of community ecology: a cavity solution to MacArthur's consumer resource model, *J. Stat. Mech.*, 033406 (2018).
[2] W. Cui, R. Marsland III, and P. Mehta, Effect of resource dynamics on species packing in diverse ecosystems, *Phys. Rev. Lett.* **125**, 048101 (2020).

- [3] M. Barbier and J.-F. Arnoldi, The cavity method for community ecology, bioRxiv: 147728 (2017).
- [4] T. Galla, Dynamically evolved community size and stability of random Lotka-Volterra ecosystems, Europhys. Lett. **123**, 48004 (2018).
- [5] A. R. Batista-Tomás, A. D. Martino, and R. Mulet, Path-integral solution of MacArthur's resource-competition model for large ecosystems with random species-resources couplings, Chaos **31**, 103113 (2021).